JOURNAL OF GEOPHYSICAL RESEARCH, VOL. 108, NO. A9, 8020, doi:10.1029/2002JA009426, 2003

FAST/Polar conjunction study of field-aligned auroral acceleration and corresponding magnetotail drivers

D. Schriver,[1] M. Ashour-Abdalla,[1,2] R. J. Strangeway,[1] R. L. Richard,[1] C. Klezting,[3] Y. Dotan,[4] and J. Wygant[5]

Received 1 April 2002; revised 8 May 2003; accepted 13 May 2003; published 5 September 2003.

[1] The discrete aurora results when energized electrons bombard the Earth's atmosphere at high latitudes. This paper examines the physical processes that can cause field-aligned acceleration of plasma particles in the auroral region. A data and theoretical study has been carried out to examine the acceleration mechanisms that operate in the auroral zone and to identify the magnetospheric drivers of these acceleration mechanisms. The observations used in the study were collected by the Fast Auroral Snapshot (FAST) and Polar satellites when the two satellites were in approximate magnetic conjunction in the auroral region. During these events FAST was in the middle of the auroral zone and Polar was above the auroral zone in the near-Earth plasma sheet. Polar data were used to determine the conditions in the magnetotail at the time field-aligned acceleration was measured by FAST in the auroral zone. For each of the magnetotail drivers identified in the data study, the physics of field-aligned acceleration in the auroral region was examined using existing theoretical efforts and/or a long-system particle in cell simulation to model the magnetically connected region between the two satellites. Results from the study indicate that there are three main drivers of auroral acceleration: (1) field-aligned currents that lead to quasistatic parallel potential drops (parallel electric fields), (2) earthward flow of high-energy plasma beams from the magnetotail into the auroral zone that lead to quasistatic parallel potential drops, and (3) large-amplitude Alfvén waves that propagate into the auroral region from the magnetotail. The events examined thus far confirm the previously established invariant latitudinal dependence of the drivers and show a strong dependence on magnetic activity. Alfvén waves tend to occur primarily at the poleward edge of the auroral region during more magnetically active times and are correlated with intense electron precipitation. At lower latitudes away from the poleward edge of the auroral zone is the primary field-aligned current region which results in the classical field-aligned acceleration associated with the auroral zone (electrons earthward and ion beams tailward). During times of high magnetic activity, high-energy ion beams originating from the magnetotail are observed within, and overlapping, the regions of primary and return field-aligned current. Along the field lines where the high-energy magnetotail ion beams are located, field-aligned acceleration can occur in the auroral zone leading to precipitating electrons and upwelling ionospheric ion beams. Field-aligned currents are present during both quiet and active times, while the Alfvén waves and magnetotail ion beams were observed only during more magnetically active events. During quiet times (no storm or substorm), the field-aligned currents were relatively weak with the resulting electron precipitation in the primary current region correspondingly weak, and for the quiescent events examined here, upwelling ion beams were not observed. The results presented here support the overall contention that processes in the magnetotail lead to field-aligned auroral acceleration and discrete aurora during active events, however, it is

[1]Institute of Geophysics and Planetary Physics, University of California at Los Angeles, Los Angeles, California, USA.
[2]Department of Physics and Astronomy, University of California at Los Angeles, Los Angeles, California, USA.
[3]Department of Physics, University of Iowa, Iowa City, Iowa, USA.
[4]Aerospace Corporation, Los Angeles, California, USA.
[5]University of Minnesota, Minneapolis, Minnesota, USA.

0148-0227/03/2002JA009426$09.00

not a single process but several processes acting at the same time and at different locations in latitude. *INDEX TERMS:* 2704 Magnetospheric Physics: Auroral phenomena (2407); 2451 Ionosphere: Particle acceleration; 2716 Magnetospheric Physics: Energetic particles, precipitating; 2753 Magnetospheric Physics: Numerical modeling; 2736 Magnetospheric Physics: Magnetosphere/ionosphere interactions; *KEYWORDS:* auroral acceleration, magnetosphere-ionosphere interactions, numerical modeling

Citation: Schriver, D., M. Ashour-Abdalla, R. J. Strangeway, R. L. Richard, C. Klezting, Y. Dotan, and J. Wygant, FAST/Polar conjunction study of field-aligned auroral acceleration and corresponding magnetotail drivers, *J. Geophys. Res.*, *108*(A9), 8020, doi:10.1029/2002JA009426, 2003.

1. Introduction

[2] The visual light display at high latitudes referred to as the aurora fascinates casual observers and researchers alike. The natural question is what causes the aurora? We know that energized electrons streaming along the Earth's ambient magnetic field and colliding with atmospheric particles produce aurora. We do not know for certain, however, how these electrons are accelerated to high energies primarily in the field-aligned direction toward the Earth, or what the drivers of this acceleration are.

[3] It has been known for some time that field-aligned accelerated precipitating electrons can cause discrete aurora. Key evidence from rocket and satellite observations made above the aurora show the presence of energetic, field-aligned electron distributions streaming earthward as well as back-scattered secondary electrons [*McIlwain*, 1960; *Hoffman and Evans*, 1968; *Hultqvist et al.*, 1971; *Frank and Ackerson*, 1971; *Rees and Luckey*, 1974; *Evans*, 1974; *Christensen et al.*, 1987]. It should be noted that discrete aurora and diffuse aurora are two different phenomena. Diffuse aurora is also caused by electron precipitation, but it results from the emptying of the loss cone of mirror bouncing plasma sheet electron distributions, which give rise to a broader, less intense aurora. The refilling of the loss cone is believed to be caused by wave-particle pitch angle diffusion at the magnetotail equator [*Kennel and Petschek*, 1966; *Kennel*, 1969]. This paper only addresses the causes of the discrete aurora.

[4] Although it is well established that energized, precipitating electrons create the discrete aurora, there are still questions regarding how these electrons achieve such energies and become focused mainly in the field-aligned direction. Presently, there are two main acceleration processes that are considered likely to occur in the auroral zone:

[5] 1. Quasistatic parallel potential drops (parallel electric fields) that can occur in regions of field-aligned current near the Earth above the ionosphere where densities are relatively low and the magnetic mirror force is relatively strong [e.g., *Knight*, 1973]. Quasistatic parallel potential drops can also form when pitch angle anisotropies (a beam and/or temperature anisotropy) in magnetotail plasma sheet distribution functions lead to differing mirror points of ions and electrons and a resulting charge separation [*Alfvén and Fälthammer*, 1963; *Persson*, 1963]. Many models of a steady state auroral electrostatic potential drop have been developed based on one or the other of these basic premises [e.g., *Lemaire and Scherer*, 1974; *Swift*, 1975; *Kan*, 1975; *Whipple*, 1977; *Chiu and Cornwall*, 1980].

[6] 2. A parallel electric field component of a kinetic Alfvén wave can develop near the Earth because of finite electron inertia [*Hasegawa*, 1976; *Mallinckrodt and Carlson*, 1978; *Goertz and Boswell*, 1979; *Lysak*, 1985]. On electron timescales this parallel field can appear quasistatic, and due to resonance and other effects can cause field-aligned electron acceleration [*Temerin et al.*, 1986; *Kletzing*, 1994; *Thompson and Lysak*, 1996].

[7] Although the two auroral acceleration mechanisms, parallel potential drops and kinetic Alfvén waves, each involve a parallel electric field, they are fundamentally different in that the former is primarily an electrostatic process, while the latter involves a propagating electromagnetic wave (albeit with a strong electrostatic component). It has been suggested that for small spatial scales electrostatic shocks might be a manifestation of an inertial Alfvén wave, however, on larger scales the two mechanisms appear to be unrelated [*Lysak*, 1998].

[8] It is likely that auroral acceleration is ultimately due to processes occurring in the magnetotail [e.g., *Frank*, 1985; *Lyons et al.*, 1999]. The basic idea is that there is a transfer of energy from earthward-propagating currents, particles, and waves that originate in the magnetotail into field-aligned plasma particles in the auroral zone via a parallel potential drop and/or kinetic Alfvén waves. It is well established that quasistatic (dc) parallel electric fields (inverted V structures and parallel potential drops) occur in regions of field-aligned current [*Mozer et al.*, 1977; *Elphic et al.*, 1998]. The field-aligned currents map into the magnetotail where they originate as part of the global magnetospheric current system [e.g., *Haerendel*, 1990]. In addition to the field-aligned currents, temperature anisotropies and beams have been observed at high altitudes above the auroral region [*Chiu et al.*, 1981; *Frank et al.*, 1981] that could also serve as drivers of quasistatic parallel electric fields in the aurora zone. The existence of a magnetotail driver for kinetic Alfvén wave auroral acceleration is supported by the recent observations of intense Poynting flux detected in a region above, but magnetically connected to the discrete auroral precipitation region. These observations clearly showed intense electron precipitation in association with field-aligned earthward propagating Poynting flux (Alfvén waves) that had oscillating magnetic and electric field components directed primarily perpendicular to the ambient magnetic field [*Wygant et al.*, 2000; *Keiling et al.*, 2001].

[9] In this paper, cause (magnetospheric driver) and effect (field-aligned auroral acceleration) are examined using data collected by the Fast Auroral Snapshot (FAST) and Polar satellites when the two satellites were in approximate magnetic conjunction. In general, FAST moved through the (northern) auroral zone between about 2000 and 4000 km altitude, while Polar passed through the (northern) auroral region at much higher altitudes, between about 4 and 8 R_E. Thus when the two satellites were on approximately coinci-

dent magnetic field lines in the northern auroral zone, Polar could determine the conditions in the near-Earth magnetotail plasma sheet at the same time that FAST was collecting data in the auroral acceleration region. There were 28 such auroral conjunction events in 1997 between May and September. Thus far seven events have been examined in detail. The results from examining these conjunction events are presented here, along with a discussion of the physical processes that lead to field-aligned auroral acceleration. These include results from a simulation model of the region between the two satellites carried out with a long-system particle in cell (PIC) code [*Schriver*, 1999, 2003]. Simulation boundary conditions at the high-altitude end of the system were set (qualitatively) for one of the events using measurements from the Polar satellite, and the simulation results were compared with observational data.

[10] The fortunate alignment and relative locations of the FAST and Polar satellites allow a thorough analysis of magnetotail/aurora cause and effect. A conjunction study was previously carried out for the auroral zone using the DE-1 and DE-2 satellites. In this case the measurement of precipitating auroral electrons at low altitudes (with DE-2), along with simultaneously observed upwelling ion beams at higher altitudes (with DE-1), indicated that a quasistatic (at least on ion timescales) parallel potential drop existed between the two satellites [*Reiff et al.*, 1986, 1988]. No attempt was made in these studies to determine a magnetotail driver of the parallel potential drop. In this study, in addition to the improved instrumentation, Polar and FAST were at near-optimum locations to determine cause and effect since FAST observed the middle of the auroral acceleration region at a few thousand kilometers altitude, whereas Polar was well above the acceleration region in the near-Earth plasma sheet (>4 R_E). By comparison, DE-2 and DE-1 were at altitudes of 400–800 and 9000–13,000 km, respectively.

[11] Seven FAST/Polar conjunction events have been examined in detail thus far. All seven events showed varying degrees of field-aligned electron precipitation in regions of field-aligned currents. Three of the events that occurred during moderate magnetically active intervals indicated that, in addition to a field-aligned current system, a magnetotail Poynting flux driver (Alfvén wave) was present. During two events with the highest magnetic activity level, a magnetotail particle beam driver (quasistatic potential drop accelerator) was also present. Four events during quiet times showed only the field-aligned current driver (quasistatic potential drop accelerator). The different drivers (field-aligned current, Alfvén waves, and magnetotail beams) were correlated with earthward electron acceleration and tailward plasma acceleration. Tailward streaming ionospheric ion beams were found in regions of strong primary (tailward directed) field-aligned currents or when the magnetotail particle flux driver was present. Upwelling electrons and ions were also detected in return current regions. During relatively quiet times, the field-aligned current was the only identifiable driver and for the events examined here only earthward accelerated electrons were detected (with relatively low energies) and there was little if any tailward streaming ions observed.

[12] Many of these results are consistent with the physics of the driver involved. For example, if low-frequency ($\sim$1 Hz) kinetic Alfvén waves are present in the auroral region, electrons would see a quasistatic parallel electric field and could be accelerated, whereas ions, due to their much larger mass, would not be accelerated in the field-aligned direction nearly as much. A strong field-aligned current or particle beam driver, on the other hand, can lead to an auroral quasistatic parallel potential drop over a time period of several seconds that can accelerate electrons earthward and ions tailward. In the return current region, a potential drop opposite of that formed in the primary current region can accelerate electrons tailward. Also, in the return current region, wave particle interactions in the auroral acceleration region can lead to transverse ion acceleration forming conic distributions, which are then accelerated tailward by the mirror force.

[13] The results of this study are presented as follows. In section 2, FAST/Polar satellite data conjunction criteria and event selection are presented, and section 3 discusses a single event in detail. Section 4 analyzes the physics of auroral acceleration discussing cause and effect relationships and simulation modeling. Section 5 summarizes all of the events examined so far, and the paper concludes in section 6.

2. Polar/FAST Conjunction Events

[14] This study examined data from measurements taken when the FAST and Polar satellites were in approximate magnetic conjunction. A list of magnetic conjunctions between FAST and Polar can be found at ftp://sierra.spasci.com/DATA/fast/prior_conjunctions_1.html, which has been compiled by William Peterson. In this list, a magnetic conjunction was defined to occur when the satellites were within 3° in invariant latitude (ILT) and within 10° in longitude. Magnetic field mapping between the two satellites was carried out using the Tsyganenko field model [*Tsyganenko*, 1989], which near the Earth uses an IGRF internal magnetic field. Figure 1 shows an example of an auroral conjunction event that occurred on 9 June 1997. The figure presents the track of the FAST satellite in red, the Polar satellite in blue-white, and the nominal auroral oval as green circles. These lines are projected onto the Earth looking down on the North Pole, and the nearest conjunction point occurred where the red and white lines cross at about 0432 UT. A two-dimensional schematic with the relative locations of the FAST and Polar flight paths near conjunction along with auroral latitude field lines is shown in Figure 2. Note that this event (9 June 1997) is discussed in detail in section 3. For all of the conjunction events examined here, the FAST satellite was located between about 2000 and 4000 km altitude, while Polar was at relatively higher altitudes between about 4 and 8 R_E (1 $R_E \approx$ 6371 km) in the Northern Hemisphere. During the single Southern Hemisphere auroral conjunction event that was found, FAST was located at about 400 km altitude and Polar at about 2.1 R_E.

[15] In 1997, FAST and Polar satisfied the conditions for a magnetic conjunction event hundreds of times. For example, during the period between 20 July and 8 September 1997, the two satellites satisfied the conjunction criteria almost 120 times. Only a select number of these events, however, occurred when the two satellites were in the

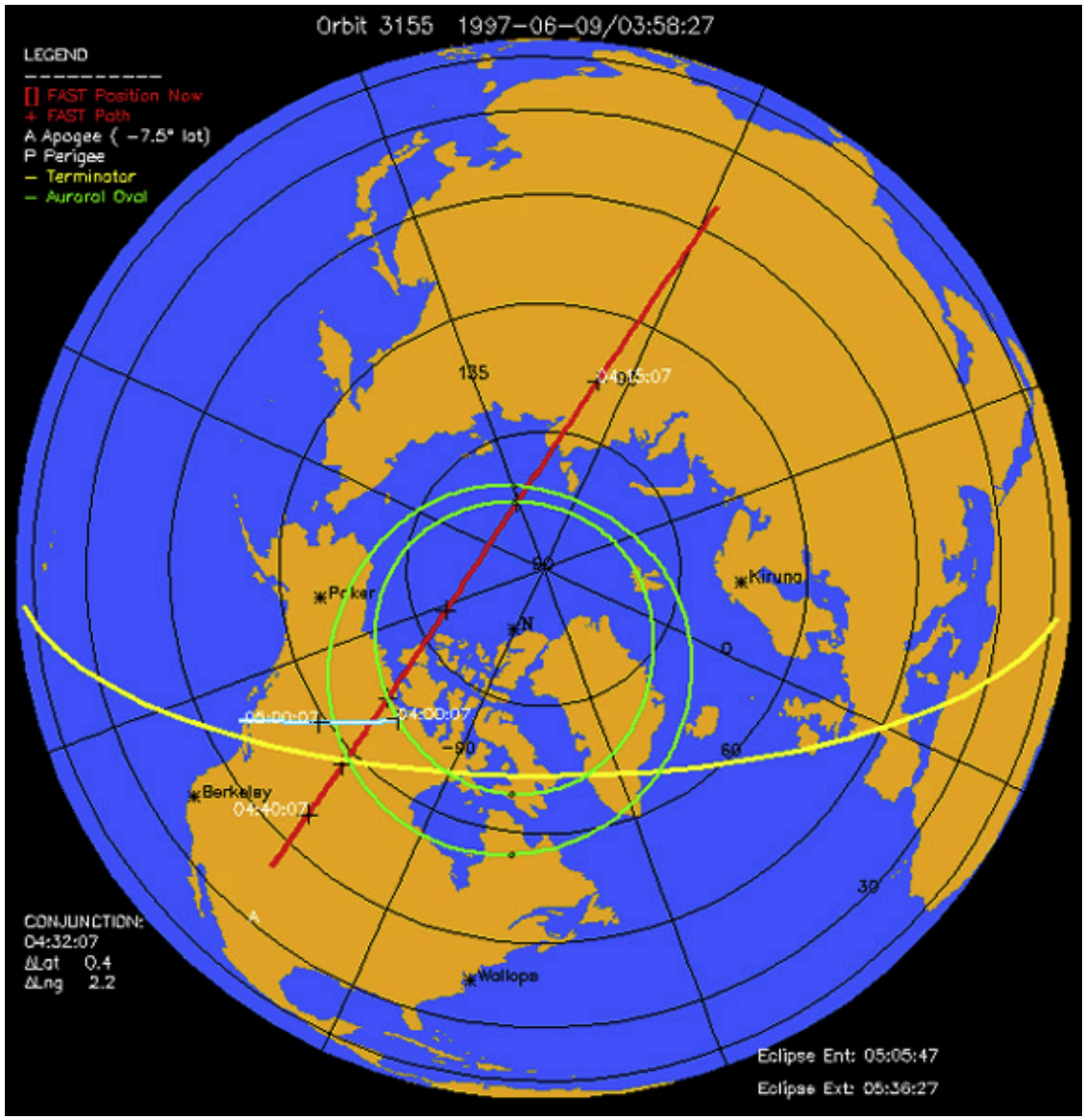

Figure 1. Projection of FAST and Polar satellite tracks onto the Earth's North Pole on 9 June 1997. The long red line is the track of FAST from about 0415 UT to 0440 UT. The shorter white (surrounded by blue) line in the bottom left quadrant shows Polar from about 0400 UT to 0500 UT. The green ovals show the nominal auroral zone and the yellow curve shows the nominal terminator. An auroral conjunction event occurs at about 0432 UT, when the FAST (red) and Polar (white) paths cross. This plot was adapted from the website at http://teams.spasci.com/conjunctions.html, which was produced using software modified by Karl Heinz Trattner at Lockheed.

closed field line region of the auroral zone, and when data were available from both satellites. Events that were not of interest to the present study, and thus were not examined, included polar cap crossings, lower latitude crossings, most Southern Hemisphere crossings, and events for which data were not available from both satellites.

[16] For this study an auroral acceleration event was selected when FAST particle data showed energetic field-aligned electrons with a net earthward flow. A description of the FAST mission can be found in the work of *Carlson et al.* [1998a]. An example of such an auroral acceleration event from 20 July 1997 is shown in Figure 3. Figures 3a and 3b show electron energy and electron pitch angle, and a somewhat sporadic group of acceleration occurrences can be seen between about 1623 UT and 1626 UT as bright red spots at 0° pitch angle (Figure 3b) with energies between about 100 and 1000 eV (Figure 3a). The direction of 0° pitch angle is field-aligned toward the Earth, while 180° is field-aligned away from the Earth. Figure 3c shows the magnetic field with the field-aligned component (b) in blue, the east-west component (e) in green, and the component transverse to these two components (o) in red. The overall increase in the east-west component (green line) indicates that the satellite is flying through a region of field-aligned current with the initial negative depression corresponding to an upward, region 2 sense current on the dawnside followed

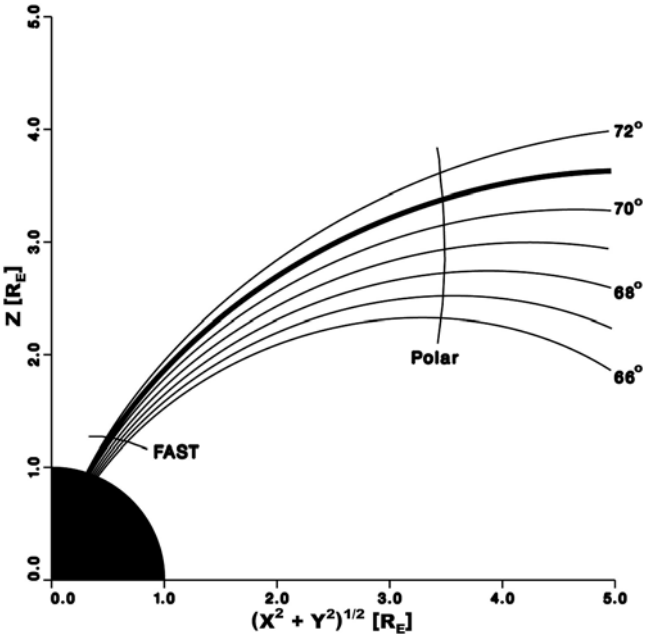

Figure 2. Schematic diagram showing the relative positions of the FAST and Polar satellites in a two-dimensional plane around the time of conjunction. GSM coordinates are used where the vertical axis is along z and the horizontal axis is along $(x^2 + y^2)^{1/2}$, both in units of Earth radii (R_E). The Earth is at the lower left and the thin black lines show the mapping of auroral latitude magnetic field lines from the Earth toward the magnetotail. The thicker black line shows the approximate location of the most poleward last closed field line. The thin curved lines show the approximate track of the FAST and Polar satellites, both of which are moving from higher to lower latitudes.

by a region 1 current directed earthward at higher latitudes. There are sharp changes imbedded in the overall current structure that shows localized smaller-scale reversals of the field-aligned current. For this event, the time at closest magnetic conjunction between FAST and Polar occurred at about 1624 UT. Events were used for this study for which FAST showed clear evidence of energetic electrons streaming earthward during near conjunctions of FAST and Polar as shown in Figure 3.

[17] Once an auroral acceleration conjunction event was identified, additional data from FAST were obtained (particle, wave, and field data), and similar data were obtained from Polar. The Hydra instrument on Polar [*Scudder et al.*, 1995] provided particle data with energies below 32 keV. For higher energies (>30 keV) particle data from the CEPPAD instrument [*Blake et al.*, 1995] were used. Electric field data [*Harvey et al.*, 1995] and magnetic field data [*Russell et al.*, 1995] from Polar were also examined, along with data from the Ultraviolet Imager (UVI) [*Torr et al.*, 1995]. Our main goal is to use particle and field data from Polar to determine what causes the earthward directed field-aligned acceleration seen at FAST altitudes. The time interval during which near conjunction occurs lasts only a second or two at most, however, data from the entire auroral crossing from both satellites were considered in our analysis. Due to the orbital characteristics and relative locations of each satellite, FAST generally passes through the auroral region in a few seconds, whereas Polar can spend up to 30 s spanning the same latitudinal region. The consideration of data from the entire auroral crossing during a conjunction event assumes a quasi-stationary ordering of auroral structure with ILT over a time period on the order of 10 s or so. This is discussed in more detail in the next section.

3. Event Case Study: 9 June 1997

[18] This section presents a single event case study to demonstrate the type of analysis carried out for the conjunction events. Data from an auroral conjunction event that occurred on 9 June 1997 will be used for this case study. It should be noted that, while other events similar to this one have been found, this event occurred near the peak of a moderate magnetic storm event with Dst at a minimum of −84 nT (as determined by the WDC-C2 KYOTO Dst index service at http://swdcwww.kugi.kyoto-u.ac.jp/dstdir/dst1/final.html). Closest to conjunction, at 0432 UT, FAST (orbit 3155) was located at about 2500 km altitude, 71° ILT, and 20.3 MLT. Polar (orbit 160) was located at 3.9 R_E altitude, 71° ILT, and 19.8 MLT. The relative locations of the two satellites for this event are shown in Figures 1 and 2.

[19] FAST data from this event are presented in Figure 4 showing electron energy and pitch angle in Figures 4a and 4b and magnetic field in Figure 4c in the same format as Figure 3. Earthward directed field-aligned acceleration is indicated in Figure 4b by the intermittent red bursts centered at 0° pitch angle from about 0431:30 UT to just after 0433 UT. The energies of the field-aligned electron bursts are about 1 keV (∼1000 eV in Figure 4a). The energy flux of the downgoing (precipitating) accelerated electrons ranges from about 1 to 10 erg cm^{-2} s^{-1}. This measured energy flux is on the order of that previously reported in auroral arcs [*Elphic et al.*, 1998; *Stenbaek-Nielsen et al.*, 1998]. Prior to about 0431:30 UT, FAST is in the polar cap, which can be inferred from the lack of high-energy electrons (>100 eV). FAST then crosses into a region of field-aligned current, as indicated by the overall increase in the east-west magnetic field component (green line, Figure 4c). Since FAST is on the duskside, the increase in east-west field component indicates a tailward directed region 1 sense current, which is labeled as FAC− between Figures 4b and 4c. Note that at the point closest to conjunction, which occurs at about 0432 UT, there is a field-aligned electron burst with energy on the order of 1 keV. The east-west magnetic field decreases after about 0432:30 UT indicating that FAST is passing through the return field-aligned current region, which is directed earthward along the terrestrial magnetic field direction and is indicated by FAC+. There are smaller-scale current structures embedded onto the overall field-aligned current system (region 1 and return current) that in some cases, but not always, correspond with the field-aligned electron bursts.

[20] The general pattern of the field-aligned currents observed by FAST in Figure 4 with respect to ILT is consistent with previous observations, whereby the primary current region (FAC−) is found at higher latitudes and the return current region (FAC+) is observed at lower latitudes [e.g., *Carlson et al.*, 1998b; *Elphic et al.*, 1998]. A close examination of the earthward streaming field-aligned bursts

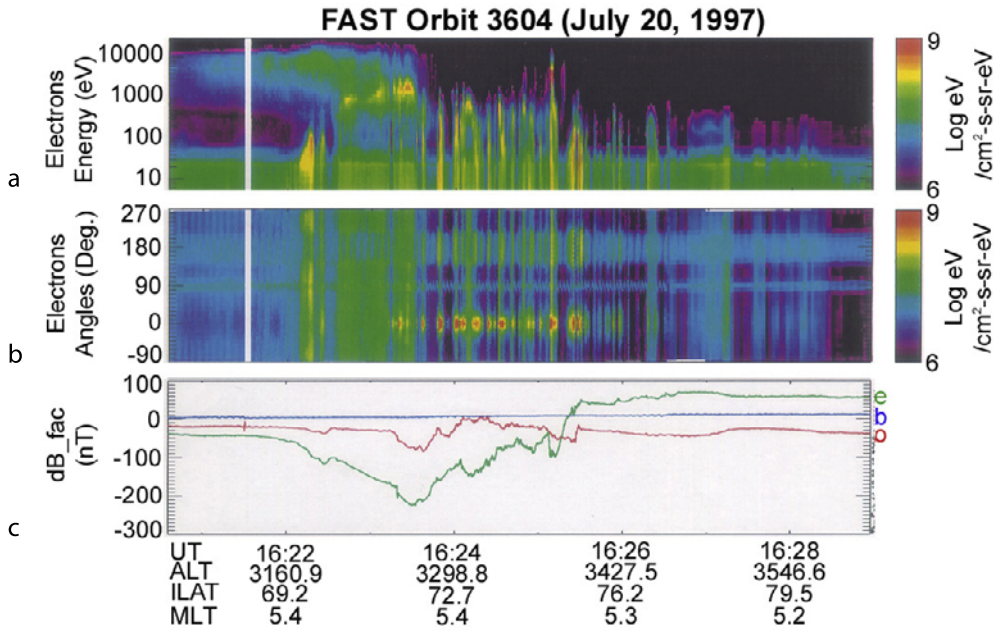

Figure 3. Data from the FAST satellite during an auroral conjunction event on 20 July 1997. (a) Shows electron energy spectra (in eV), (b) electron pitch angle with 0° corresponding to the earthward direction and 180° away from the Earth, (c) shows the magnetic field components (in nT) in the east-west direction (green e trace), the field-aligned direction (blue b trace), and the direction transverse to e and b (red o trace). Earthward directed electron flux events are evident between about 1623 and 1626 UT as a series of red bursts at 0° pitch angle in Figure 3b.

within the field-aligned currents as determined from the magnetic field in Figure 4, however, shows several interesting features that will be important when looking at the magnetospheric drivers with Polar. One feature is that at the very poleward edge of the auroral zone at ~0431:30 UT, the most intense electron precipitation occurs. At slightly lower latitudes in the upward directed region 1 current (FAC−), until about 0432:40 UT, the field-aligned electrons are not continuous in the larger-scale current structure, but are bursty. Another important point to be made is that energetic field-aligned earthward streaming electrons are observed well into the return current region (FAC+ after ~0432:40 UT) where the field-aligned current is directed earthward. It should be noted that the intermittent bursts of earthward accelerated electrons are a common feature in the electron data and have been seen in other auroral conjunction events (e.g., Figure 3).

[21] The electron data shown in Figure 4 clearly indicate that electrons have been accelerated earthward in the field-aligned direction at some location above the FAST satellite. An example of an electron distribution function nearest conjunction (~0432 UT) is presented in Figure 5, which shows distribution contours plotted in the perpendicular direction (vertical) and parallel direction (horizontal). Positive parallel velocities correspond to the earthward direction. The most obvious feature is the elongation of the velocity contours in the parallel earthward direction, corresponding to the peak at 0° pitch angle seen in Figure 4. It is interesting to note that, even though there is clearly a net electron flow in the earthward direction along the magnetic field, there is no distinct beam present in the distribution. This is probably because the electrons are preferentially accelerated in the field-aligned direction at some location above the satellite and form a beam, which then excites plasma waves that smear the original beam distribution via wave-particle interactions. Electric field spectra at this time (not shown) indicate the presence of electrostatic oscillations near the upper hybrid frequency, which would be consistent with an electron beam driven instability. Although beam-generated waves in the auroral zone are themselves interesting, they are not within the scope of the present paper.

[22] The goal of this study is to determine the field-aligned acceleration mechanisms and the corresponding magnetotail drivers associated with this acceleration. To this end we now look at Polar data for this event, which was located above FAST along approximately the same magnetic field lines at about 3.9 R_E altitude. We start by looking at magnetic and electric field data from Polar around the time of the conjunction. Figure 6 shows the magnetic field data observed during the time interval between 0420 UT and 0440 UT on 9 June 1997. Figure 6a shows three colored lines, which are the dB_x (blue), dB_y (red), and dB_z (green) residual magnetic field components subtracted from the 1996 Tsyganenko field model [*Tsyganenko and Stern*, 1996] in GSM coordinates. Figure 6b shows the E_z electric field component normal to the spin plane, which corresponds approximately to the north-south direction in GSE coordinates. It can be seen in Figure 6 that the field profiles are relatively smooth prior to about 0423 UT. At 0423 UT there are strong oscillations in the magnetic and electric fields followed by a sharp decrease in the dB_x field component (blue trace) until about 0428:30 UT. After this time a gradual overall increase in dB_x occurs. Note that after

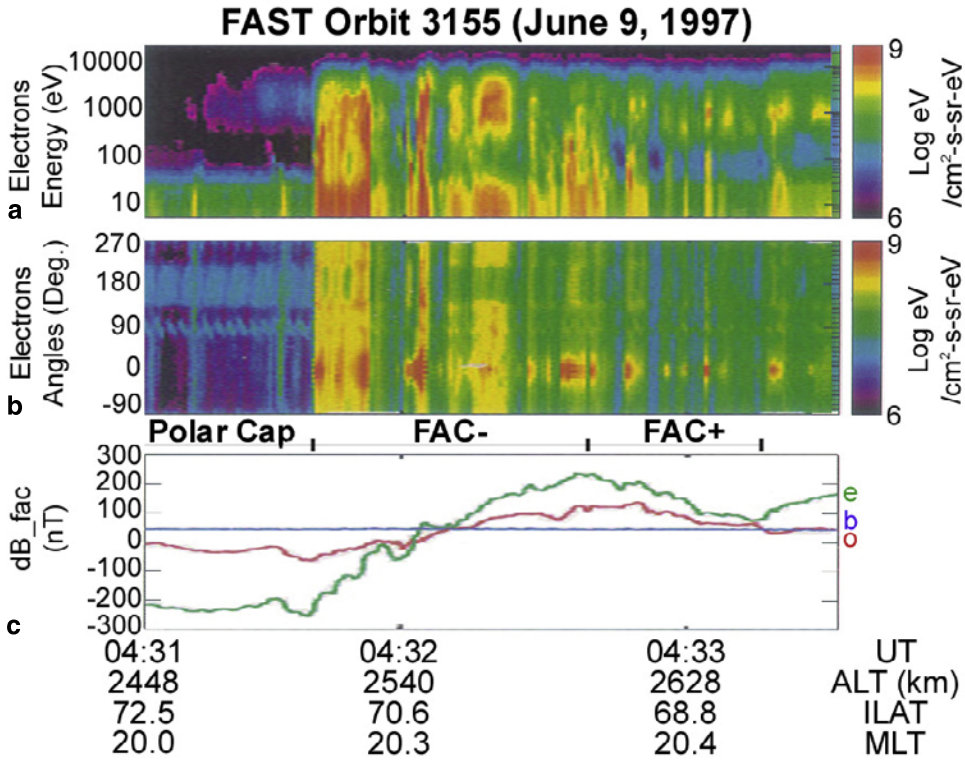

Figure 4. FAST data are shown for the auroral conjunction event on 9 June 1997. The format is the same as Figure 3 showing electron energy and pitch angle in (a and b) and the magnetic field in (c) with the field-aligned component (b) in blue, the east-west component (e) in green, and the component transverse to these two components (o) in red. For this event FAST, going from high to lower latitudes, crosses from the polar cap into the auroral region at about 0431:30 UT as evidenced by the sudden appearance of high-energy electrons (Figure 4a) and the change in the east-west magnetic deflection (green line, Figure 4c). From 0431:30 UT until about 0432:40 UT, FAST passes through a region of net field-aligned current pointing tailward (labeled FAC−) consistent with a region 1 current on the duskside. After 0432:40 UT, FAST then goes through a gradual region of return current (labeled FAC+). Bursts of field-aligned energized electrons occur intermittently when FAST is in the auroral zone as seen by the (red) peaks in 0° pitch angle in Figure 4b.

about 0425 UT the electric field (Figure 6b) is relatively smooth just above 0 mV m^{-1}.

[23] The magnetic and electric field data indicate that Polar is positioned in the polar cap region at higher latitudes prior to 0423 UT and then moves to lower latitudes crossing into a region of field-aligned current after 0423 UT. The decreasing dB_x indicates that the field-aligned current is directed away from the Earth (indicated by FAC− at the top of Figure 6), which is consistent with a region 1 current system. After about 0428:30 UT, Polar crosses into the return current region where the field-aligned current is directed earthward, as seen by the gradual increase in dB_x and indicated by FAC+ at the top of Figure 6. This field-aligned current system is consistent with the field-aligned current system observed at lower altitudes by the FAST satellite (Figure 4). At Polar the field-aligned current density ($j_{\|}$) is estimated to be about 0.8 μA m^{-2} (assuming $\Delta B_x \sim$ 60 nT and Δy = 50 km), while at FAST $j_{\|}$ is between about 10 and 50 times greater than at Polar (depending on the cross-field distance). This is consistent with a field-aligned current sheet that increases with the terrestrial magnetic field keeping $j_{\|}/B$ approximately constant when mapped from Polar to FAST. Also, qualitatively similar to the FAST observations are the smaller-scale magnetic field structures embedded in the overall field-aligned current systems.

[24] An outstanding feature of the magnetic and electric fields in Figure 6 (in addition to the field-aligned current systems) are the strong fluctuations that occur between about 0423 UT and 0425 UT. The fluctuations have a period less than 1 min and for an electric field fluctuation amplitude of $\delta E \approx 20$ mV m^{-1}, and a magnetic field fluctuation amplitude of $\delta B \approx 15$ nT, the $\delta E/\delta B$ ratio is $\sim$1300 km s^{-1}. This gives a phase speed comparable to the local Alfvén speed, which is about 1000–2000 km s^{-1} (using measured key parameter values at 0424 UT of 10 cm^{-3} for the density of a mixed hydrogen-oxygen plasma and 425 nT for the total ambient magnetic field). This implies that the fluctuations correspond to an Alfvén wave, and a calculation of the Poynting flux $\mathbf{S}_{\|}$ (where $\mathbf{S}_{\|}$ is proportional to $\delta\mathbf{E} \times \delta\mathbf{B}$) shows that the field-aligned component is propagating earthward with an energy flux value of 0.5–1 erg cm^{-2} s^{-1}. Such observations are similar to Alfvén waves previously seen by the Polar satellite in regions above the auroral zone [*Wygant et al.*, 2000; *Keiling et al.*, 2001]. This earthward propagating Poynting flux is amplified as it moves toward the Earth in proportion to the

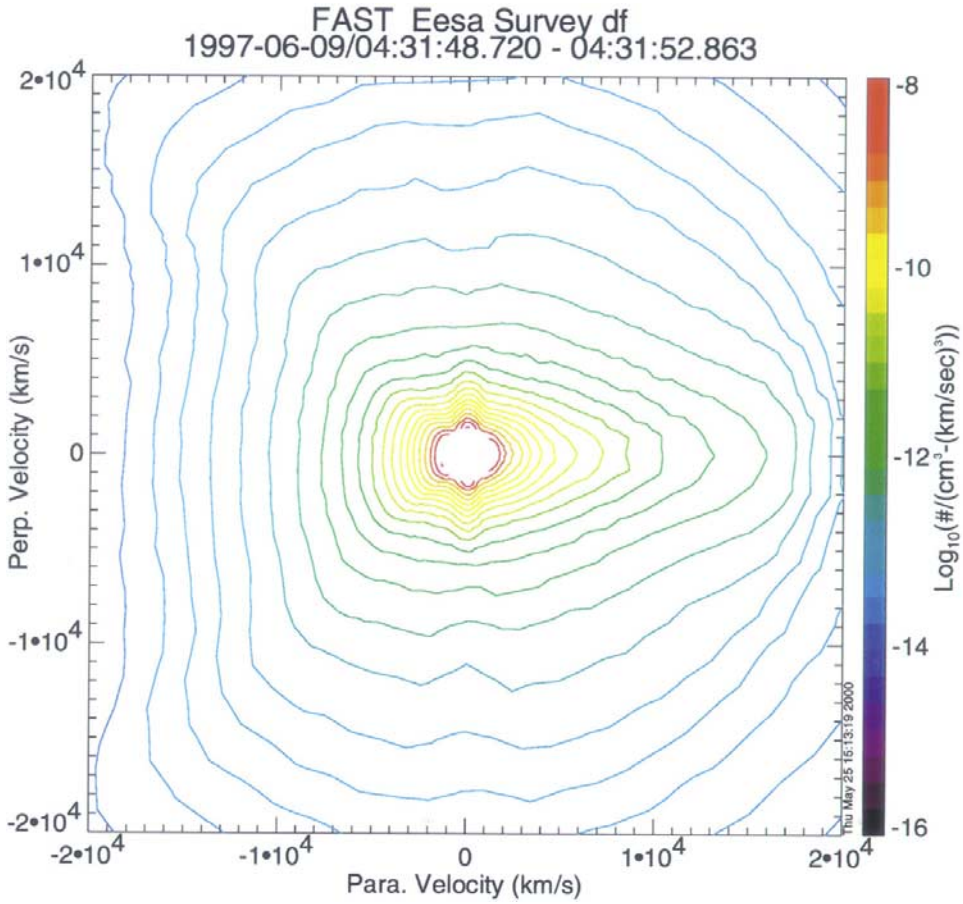

Figure 5. Electron distribution function taken for the conjunction event shown in the previous figure on 9 June 1997 at around 0432 UT. Velocity space contours are shown with the perpendicular velocity being along the vertical axis in km s^{-1} and the parallel velocity along the horizontal axis (also in km s^{-1}). The contours are elongated in the positive parallel direction, which corresponds to the direction toward the Earth, indicating that there is a net earthward flux of electrons. Such a feature corresponds to a peak in 0° pitch angle as seen in Figure 4b.

increasing magnetic field [*Wygant et al.*, 2000], and if mapped to the ionosphere, would have an energy flux on the order of 100 erg cm^{-2} s^{-1}. The energy flux of these intense waves is quite significant and clearly represents a driver of field-aligned auroral acceleration and resulting electron precipitation. It should be noted that for the event here (and others that have been examined) the earthward-propagating Alfvén waves are confined to the most poleward edge of the high-altitude auroral zone, and at lower latitudes the electric field fluctuations are near zero (for example after about 0425 UT in Figure 6).

[25] The large-amplitude Alfvén waves observed by Polar between 0423 UT and 0425 UT occur at the poleward edge of the near-Earth plasma sheet at about 71° ILT. FAST crosses into the auroral zone just after 0431:30 UT, which is also at about 71° ILT, and sees intense electron precipitation at low altitudes. The time difference between when the two satellites cross the region of 71° ILT is about 7 s or so, which clearly does not qualify as a conjunction. The data, however, suggest that the Alfvén waves emanating from the magnetotail persist at least as long as 7 s (0424 UT to 0431 UT) and accounts for the electron precipitation observed by FAST. A strong correlation has been made previously between Alfvén waves observed by Polar (usually at the poleward edge of the near-Earth plasma sheet) and intense electron precipitation using the UVI instrument onboard Polar [*Wygant et al.*, 2000]. Although FAST was not in the auroral zone at 0425 UT to observe electron precipitation directly, UVI images from Polar at 0425 UT show intense electron precipitation at the poleward edge of the auroral oval. The UVI images show this precipitation persisting at about the same latitudinal location at least until 0432 UT, when FAST observes electron precipitation. UVI data are presented and discussed later in this section.

[26] We now look at particle data during the same time interval from the Polar satellite Hydra instrument in Figure 7. Electron data are given in Figures 7a and 7b that show the electron energy and electron skew. The skew is the difference in count rate between the field- and the antifield-aligned particles normalized to one-sigma error. Thus the skew is a measure of the significance of the difference between the 0°–30° and 150°–180° pitch angle bins. The skew diagrams are color-coded red for field-aligned earthward directed flow and blue for field-aligned tailward directed flow. Figures 7c and 7d give the ion energy and skew in the same format as the electrons. After about

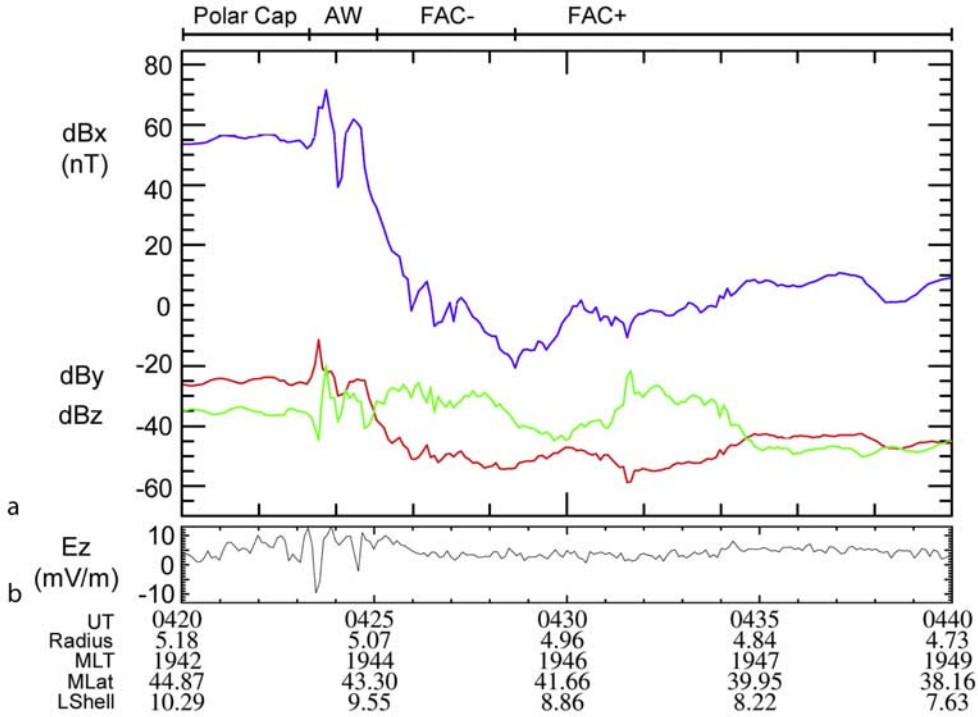

Figure 6. Data from the MFE magnetic field instrument (courtesy of C. Russell) and from the EFI electric field instrument (courtesy of F. Mozer) on the Polar satellite are shown for the time interval from 0420 UT to 0440 UT on 9 June 1997. (a) The dB_x (blue line), dB_y (red line), dB_z (green line) residual magnetic field components in GSM coordinates are shown where the field is subtracted from the field model of *Tsyganenko and Stern* [1996]. The E_z electric field component approximately in GSE coordinates is shown in Figure 6b. When the Polar satellite crosses from the polar cap (open field lines) into the near-Earth plasma sheet at about 0423 UT, there are large fluctuations in both the magnetic and electric fields associated with a large-amplitude Alfvén wave (labeled AW above Figure 6a). After about 0425 UT, dB_x (blue line) strongly decreases which indicates that the satellite is passing through a region of field-aligned current directed tailward (FAC−) associated with a region 1 current. A modest increase in dB_x after about 0428 UT implies that the satellite is going through the return current region, which is directed earthward (labeled FAC+).

0423 UT the electrons (Figure 7a) are relatively energetic (>1 keV), which indicates that the satellite has crossed from the polar cap into the near-Earth plasma sheet boundary layer (PSBL). The PSBL is a transition region between the open field line, high-latitude lobe that maps to the polar cap and the plasma sheet on closed field lines that map from the magnetotail to the auroral zone [*Eastman et al.*, 1984]. The electron skew (Figure 7b) is quite variable during the interval, however, there is some indication of earthward directed electron flow at high latitudes at around 0425 UT and tailward flowing electrons at around 0429 UT and at 0435 UT in the return current region at lower latitudes. The distribution function that corresponds to the upflowing electrons at 0435 UT (not shown) is consistent with similar types of upflowing electrons observed previously by Polar above the auroral region [*Kletzing and Scudder*, 1999].

[27] The ions observed by Polar during this time interval (Figures 7c and 7d) show two distinct populations with different energies. One of these ion populations can be seen at about 1 keV in the ion skew plot (Figure 7d) as dark blue patches from 0426 UT to 0428 UT and again from about 0431 UT to 0434 UT. The skew (∼100) of this ion population is oriented tailward and indicates upwelling ions (ion distribution functions are shown in the next figure) originating from below the satellite in the auroral region. Data from the Toroidal Imaging Mass-Angle Spectrometer (TIMAS) instrument onboard Polar show that this upwelling population consists primarily of O^+ ions, which is a clear indicator that this population is of ionospheric origin. The second ion population has relatively higher energies between ∼3 and ∼32 keV (upper energy limit of the instrument), and represents a warm background plasma. In particular, there is a series of green-yellow bands in Figure 7c starting from about 0430 UT to 0440 UT that show a decreasing energy profile with time. These ions are mainly H^+ (from TIMAS) and their energies (>1 keV) are consistent with PSBL plasma energies [e.g., *Frank*, 1985; *Baumjohann et al.*, 1989]. The skew of the higher-energy H^+ population (yellow regions at high energies in Figure 7d) shows an earthward directed flow, indicating that it originates from the magnetotail.

[28] The distinct nature of the upwelling ion populations can be seen more clearly in Figure 8, which shows distribution functions at three different times at the top of the figure. The ion skew is included below the distributions for reference in the same format as in Figure 7d. In each of the

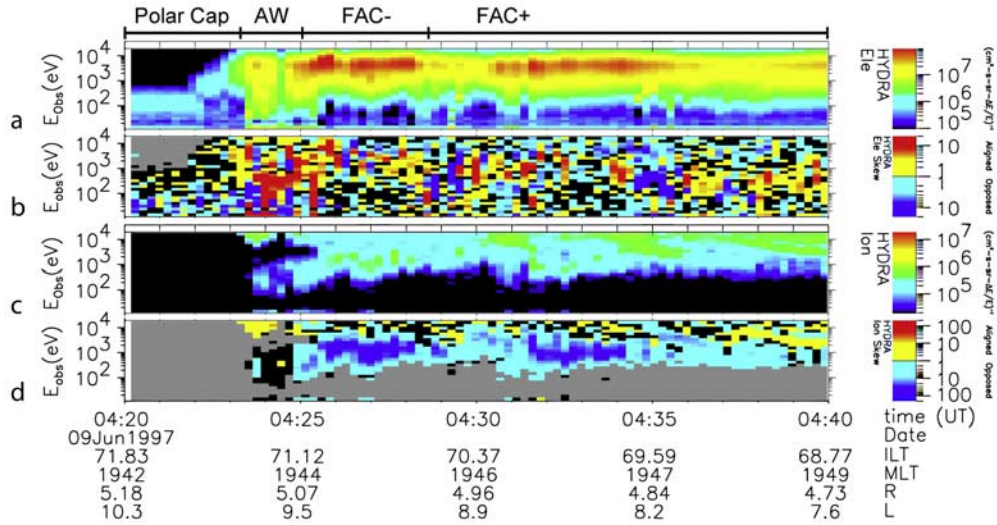

Figure 7. Polar particle data from the Hydra instrument are shown for the auroral conjunction event on 9 June 1997 from 0420 UT to 0440 UT. Electron data energy spectra (in eV) and skew are shown Figures 7a and 7b, respectively. The same quantities for ions are shown in Figures 7c and 7d. The skew is the difference in count rate between the field-aligned and the antifield-aligned particles. It is normalized to the one sigma error and thus gives a sense of the net field-aligned flow either toward the Earth (yellow-red) or away from the Earth (green-blue). Ion flow away from the Earth is seen in the bottom panel as dark blue regions at about 1 keV from about 0426 UT to 0428 UT and again from about 0431 UT to about 0436 UT. At higher energies (>10 keV) there are indications of an earthward ion flow (yellow) also seen in Figure 7d. In Figure 7b, earthward directed electron flow can be seen at about 0425 UT (red patches) and tailward directed electron flow can be seen at about 0429 UT and 0435 UT (dark blue patches).

distribution function plots, the horizontal axis is in the field-aligned direction with positive right toward the Earth and negative left toward the magnetotail, and the vertical axis is transverse to the ambient magnetic field. The distribution function at the left is taken at 0427 UT when Polar is at higher latitudes in the primary field-aligned current region (labeled FAC−), and it clearly shows a tailward drifting O^+ beam with a tailward drift speed of about -100 km s^{-1} (corresponding to a drift energy of ∼1.7 keV). Energetic upwelling ions are a common feature of the high-altitude auroral region [*Shelley et al.*, 1976; *Ghielmetti et al.*, 1978; *Gorney et al.*, 1981; *Reiff et al.*, 1988] and are an indication of a field-aligned acceleration process at a location below the Polar satellite. Figures 8b and 8c show distribution functions taken in the return current region (FAC+). Figure 8b taken at 0432 UT shows a well-formed magnetotail directed ion beam

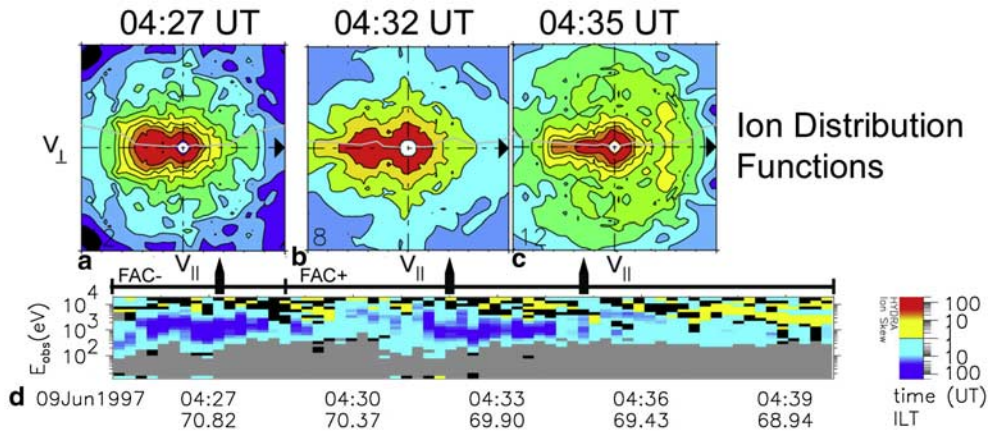

Figure 8. Ion distribution functions from the Hydra instrument are shown at three different times at 0427 UT (a), 0432 UT (b), and 0435 UT (c) for the 9 June 1997 event. Parallel velocity is along the horizontal direction with negative velocities (to the left of center) corresponding to tailward flow and positive velocities (to the right of center) is in the earthward direction. Transverse velocity (to the ambient magnetic field) is along the vertical direction. The continuous ion energy skew is shown for reference below the distribution functions in the same format as Figure 7.

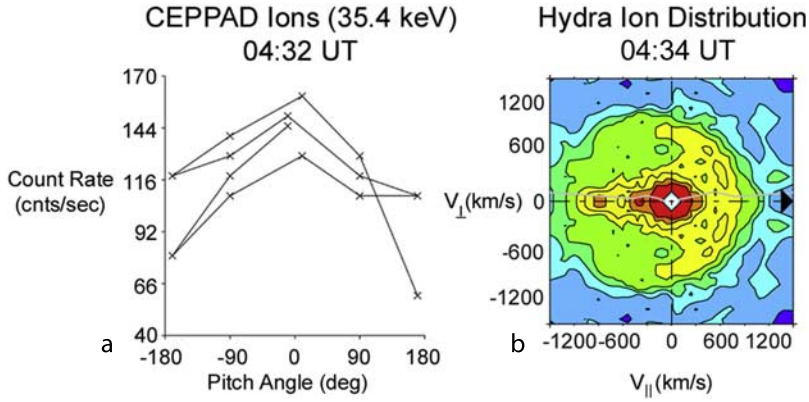

Figure 9. Ion data from Polar for the 9 June 1997 event is shown for the CEPPAD instrument at 0432 UT (a) and from the Hydra instrument at 0434 UT (b). The Hydra data on the right show an ion distribution function in the same format as shown in Figure 8 whereby transverse velocity (to the ambient magnetic field) is along the vertical direction and parallel velocity is along the horizontal direction with positive parallel velocity (to the right of center) in the earthward direction. For Figure 9a from CEPPAD, count rate versus pitch angle is shown where 0° is toward the Earth and 180° is away from the Earth. Data in this figure are shown from the 35.4 keV energy channel. Peaks in the count rate occur when the pitch angle is field-aligned toward the Earth (0°), and minima tend to occur in the antiearthward direction (180°). This trend is also present in other energy channels from about 15 keV to about 65 keV, with a peak in the 35 and 45 keV energy channels.

distribution function that is very similar in form compared with the beam found in the primary current (FAC−) region at 0427 UT. The distribution function in Figure 8c is taken at 0435 UT and shows upwelling ions, but in this case the distribution has a flat extension toward negative tailward velocities and is not beam-like compared to the other two distributions. The different types of upwelling distribution functions indicate different physical mechanisms for their formation. The upwelling beams would be expected for ions moving through a quasistatic parallel potential drop somewhere below the Polar satellite. The flat upwelling ion distribution would form as a result of transverse ion acceleration due to wave-particle interactions occurring below the satellite forming an ion conic and then the mirror force folding the ions in pitch angle toward parallel velocities as the distribution function moves away from the Earth [e.g., *Sharp et al.*, 1977]. Note that after the initial transverse heating by wave-particle interactions, the mirror force changes only the pitch angle and thus such an upwelling ion distribution formed in this way would not resemble a beam, but a distribution elongated in the parallel tailward direction as seen in Figure 8c.

[29] The distribution function on Figure 8a is expected since in the primary field-aligned current (FAC−) a potential drop forms at auroral altitudes below Polar leading to the observed upwelling beam. The distribution function on Figure 8c is consistent with the return current region (FAC+) since it has been shown that electron beam driven wave-particle interactions at auroral altitudes are associated with ion conics [*Carlson et al.*, 1998b], which would then lead to an upwelling mirror folded distribution at higher altitudes. One would not expect, however, a well-defined, upwelling ion beam in the nominal return current region as seen in Figure 8b. Recall that the FAST data at low altitudes (Figure 4) showed instances of energetic precipitating electrons within the return current region. These results taken together indicate the presence of a field-aligned potential drop formed within the return current region in the auroral zone that accelerates electrons earthward and ions tailward. A possible driver of this parallel potential drop is a high-energy (>10 keV), earthward streaming magnetotail ion population. As already noted in Figure 7, a dispersed high-energy (>10 keV) earthward drifting ion population of magnetotail origin is present between about 0430 and 0435 UT in approximate coincidence with the upwelling ion beams seen at Polar.

[30] To further examine the properties of the earthward streaming high-energy ions, two distributions are presented in Figure 9, which shows ion data from the Polar CEPPAD instrument at 0432 UT in Figure 9a and an ion distribution function from Hydra at 0434 UT in Figure 9b. Data from CEPPAD, which has ion energy channels from 15 keV up to 1500 keV, are used since for much of the event shown in Figure 7, the higher ion energies go above the Hydra instrument energy cutoff of about 30 keV. Figure 9a shows ion count rate versus pitch angle from the CEPPAD 35.4 keV energy channel and it can be seen that the pitch angle peaks at about 0°, which corresponds to an earthward directed flow. This feature is seen in other energy channels, and an analysis of five different CEPPAD energy channels (15.6 keV up to 65.2 keV) indicates that there is an earthward flowing ion distribution with a peak energy between about 35 and 45 keV. The Hydra distribution function taken at 0434 UT on Figure 9b shows a kidney-bean shaped ion (H^+) population with a parallel earthward drift speed of about 600 km s^{-1} (peak energy of about 3.7 keV). The ion distributions in Figure 9 are typical of the type of anisotropic earthward streaming field-aligned ion beam distributions observed further down the magnetotail in the PSBL [*Hones et al.*, 1972; *Frank et al.*, 1976; *DeCoster and Frank*, 1979; *Eastman et al.*, 1984; *Takahashi and Hones*, 1988]. The PSBL ion beams have a velocity

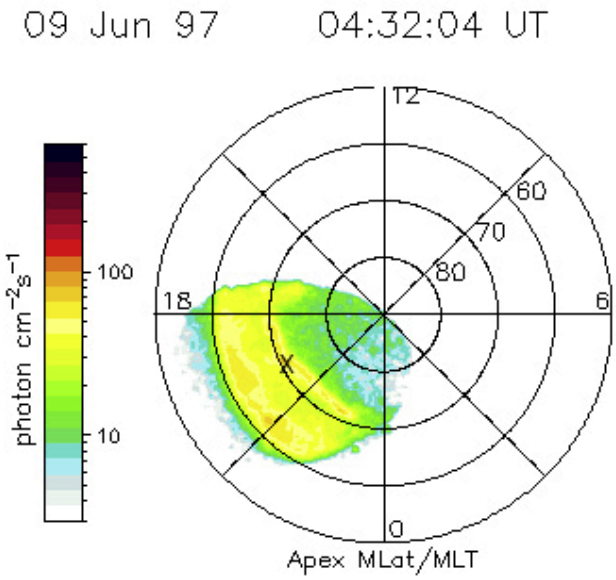

Figure 10. Data from the UVI instrument on the Polar satellite (courtesy of G. Parks) is shown for the 9 June 1997 conjunction event at 0432 UT. Auroral enhancements can be seen between about 60° and 70° latitude. The FAST/Polar conjunction field is mapped to the point on the Earth indicated by the cross, near about 70° latitude, and 20 MLT.

dispersion signature such that the beam speed decreases with decreasing latitude toward the central plasma sheet [*Forbes et al.*, 1981; *Takahashi and Hones*, 1988]. At the highest latitudes the PSBL ion beam energy is at its highest and ion beam streaming energies up to 60 keV have been detected at the most lobeward edge of the PSBL [*Möbius et al.*, 1980; *Schriver et al.*, 1990]. The earthward streaming PSBL ion beams can act as a driver for auroral acceleration and it has been shown that these beams can lead to the formation of a quasistatic parallel potential drop in the auroral zone [e.g., *Serizawa and Sato*, 1984; *Schriver*, 1999]. This will be discussed further in the next section.

[31] We now estimate the energy flux carried by the earthward directed PSBL ion beams for the two different distributions shown in Figure 9. For the ion beam at 0434 UT from Hydra (Figure 9b), the energy flux is about 0.1 erg cm^{-2} s^{-1}. For the ion beam at 0432 UT (Figure 9a) the energy flux is estimated to be about 0.5–5 erg cm^{-2} s^{-1} for a beam drift energy of 40 keV and a beam density between 0.04 and 0.4 cm^{-3}. The energy flux must be estimated in the latter case since unlike Hydra, CEPPAD does not routinely calculate the energy flux. The biggest uncertainty in the energy flux calculation for CEPPAD is the density of the beam. For example, at 0432 UT, key parameter data show an electron density on the order of ~1.0 cm^{-3} and TIMAS key parameter data show that the low-energy O^+ density is about 0.6 cm^{-3}. The question to consider is how much of the high-energy H^+ makes up the beam and how much makes up the background. Assuming a PSBL H^+ beam with density of up to one tenth of the total H^+ density, the beam density is somewhere between 0.04 and 0.4 cm^{-3}.

[32] To get an indication of the auroral activity occurring at the Earth during this event, we now show data from the UVI instrument onboard Polar. A plot with a view looking down onto the North Pole region of the Earth is shown in Figure 10 at a time nearest conjunction (0432 UT). The cross in Figure 10 shows the approximate location on the Earth to which the FAST/Polar locations would magnetically map on the duskside just above 70° latitude. Enhanced auroral emissions are evident around this location, indicating enhanced electron precipitation at this time. The energy flux associated with these auroral emissions can be estimated from Figure 10 by dividing the scale, which shows photons cm^{-2} s^{-1}, by 4 [*Wygant et al.*, 2000]. With this estimate we can determine that the region with enhanced auroral emissions around conjunction has an energy flux that ranges from about 5 to 15 erg cm^{-2} s^{-1}.

[33] We now summarize the data from both the FAST and Polar satellites for the conjunction event on 9 June 1997 characterized in latitude from most poleward (higher latitudes) toward the equator (lower latitudes).

[34] 1. High-latitude edge of the auroral zone: A Poynting flux due to fluctuating magnetic and electric fields (Alfvén wave) was observed at an altitude of 3.9 R_E propagating earthward with an energy flux of about 0.5–1 erg cm^{-2} s^{-1}. Strong electron precipitation and intense auroral brightening occurred during the time the Alfvén waves were observed.

[35] 2. High-latitude auroral zone: Away from the most poleward edge, tailward directed field-aligned current (region 1 sense or primary current) was observed at both low (~2500 km) and high (3.9 R_E) altitudes. The field-aligned current had sharp, small-scale variations embedded in the overall field-aligned current structure. A series of bursty earthward streaming field-aligned directed electrons with energies of ~1 keV were detected at about 2500 km with an energy flux of about 1–10 erg cm^{-2} s^{-1}. Upwelling field-aligned O^+ beams of ionospheric origin with an energy of ~1 keV were observed streaming away from the Earth at 3.9 R_E altitude.

[36] 3. Midlatitude to lower-latitude auroral zone: A tailward directed, field-aligned return current extending equatorward in latitude was observed at both high (3.9 R_E) and low (~2500 km) altitudes. At midlatitudes within this region, tailward streaming ionospheric origin O^+ beams with energy of ~1 keV were observed at 3.9 R_E at approximately the same latitudes as higher-energy (~4 keV up to 40 keV) field-aligned H^+ beams of magnetotail origin. The energy flux of the earthward streaming beams was estimated to be about 0.1–5 erg cm^{-2} s^{-1}. At lower latitudes within this region an upwelling tailward directed electron beam with energy of ~400 eV was observed at 3.9 R_E in approximate coincidence with upwelling ion distributions resembling mirror folded ion conics.

[37] In general, strong auroral emissions were observed in the Earth's ionosphere at locations that magnetically mapped to the FAST/Polar locations of the satellites as they passed through the auroral region. The latitudinal structure observed for this event is consistent with previous observations in that Alfvén waves are usually found at the most poleward latitudes [*Wygant et al.*, 2000], and then with decreasing latitude the primary and return field-aligned current regions are detected, respectively [e.g., *Carlson et al.*, 1998a, 1998b].

[38] The observations for this event allow some basic conclusions to be drawn. At the high-latitude edge of the

auroral zone, Alfvén waves dominate the physics of the region causing strong field-aligned electron acceleration and precipitation. In the primary current region at latitudes just equatorward of the Alfvén layer, a field-aligned acceleration mechanism was operating at altitudes between FAST (2500 km) and Polar (3.9 R_E). This mechanism, likely in the form of a parallel potential drop, accelerated electrons earthward and O^+ ions tailward with both species having about the same streaming energy ($\sim$1 keV). In the return current region at lower latitudes, electrons were accelerated tailward, probably by a parallel potential structure reversed compared to the primary current region [*Carlson et al.*, 1998b], and upwelling ions in the form of mirror-accelerated ion conics were observed at high altitudes. At latitudes somewhat in between the primary and return current region, high-energy PSBL ion beams streaming earthward were observed in coincidence with electron precipitation and tailward accelerated ionospheric ion beams, suggesting that a parallel potential drop was formed at auroral altitudes along these field lines. Thus three magnetospheric drivers of auroral acceleration have been identified at high altitudes acting at the same time but at different latitudes: (1) field-aligned currents, (2) earthward streaming PSBL ion beams, and (3) earthward propagating Alfvén waves. We now consider each of these magnetotail drivers.

4. Physics of Field-Aligned Auroral Acceleration

[39] The magnetospheric drivers discussed in the previous section were all associated with field-aligned acceleration of electrons and ions in the auroral zone. We now discuss the physics of each driver as they relate to auroral acceleration.

4.1. Field-Aligned Current/Quasistatic Potential Drops

[40] It is well known on a global level that field-aligned currents form between regions of the magnetotail or magnetopause and the Earth's ionosphere [e.g., *Iijima and Potemra*, 1976]. The field-aligned currents originate in the magnetotail convection current sheet or the magnetopause flanks, possibly as a result of flow vortices or some other mechanism [*Vasyliunas*, 1983], flow along magnetic field lines into the Earth's ionosphere, move across the polar cap, and then return to the magnetotail. Although the precise locations and pattern of this global current structure are still being examined, there is conclusive evidence that field-aligned currents flow between the magnetosphere and the ionosphere, and that these field-aligned currents are usually located at high latitudes in coincidence with the auroral region. The event study in the previous section provides an example of such field-aligned currents in the auroral zone.

[41] In the primary field-aligned current region near the Earth, where the magnetic mirror force strengthens, a quasistatic potential drop can form with a particular current-voltage relationship [*Knight*, 1973]. For typical plasma populations in the cold, dense ionosphere and the hot, less dense plasma sheet, potential drops of several kilovolts are possible. It should be noted, however, that the current-voltage relationship of Knight does not indicate exactly where the potential drop should form or its extent along the terrestrial magnetic field in the auroral region. Nevertheless, to maintain current flow between the plasma sheet and the ionosphere, strong localized potential drops can form in the primary current region of the auroral zone [e.g., *Ergun et al.*, 2000] causing field-aligned electron acceleration toward the Earth and upwelling ion beams away from the Earth.

[42] The event study of the previous section showed the presence of a region 1 sense, primary field-aligned current at higher auroral latitudes. The parallel current density in this region was calculated to be about 0.8 μA m^{-2} at Polar, which was located at about 3.9 R_E altitude. Earthward streaming field-aligned electrons observed at FAST ($\sim$2500 km altitude), which had similar streaming energies as tailward streaming O^+ beams seen at Polar, implies that a potential drop was formed between the satellites. The potential drop ($\Delta\phi$) can be estimated using the relationship of *Knight* [1973] as follows:

$$\Delta\phi = \frac{j_{\parallel}\sqrt{2\pi mkT}}{q^2 n},$$

where m is the electron mass, n is the electron density, and T is the electron temperature. At Polar, which is in the near-Earth extension of the hot, tenuous magnetotail plasma sheet, the electron density was about 1 cm^{-3} and the electron temperature was about 1000 eV. Using these observed values for n, T and $j_{\parallel}$ from Polar give a potential drop of $\Delta\phi \sim 950$ V. This is consistent with the energy of the earthward streaming electrons observed at FAST and the tailward streaming O^+ beams observed at Polar, both of which had streaming energies of about 1000 eV.

[43] The field-aligned potential drop that forms due to a field-aligned current is essentially a double layer, which is defined as consisting of two equal but opposite space charge layers with a potential that varies monotonically through the layer [*Block*, 1972, 1978]. The spatial extent of the double layer depends on the local plasma conditions. Double layers can form in a current-driven plasma at the site of a density depression [*Carlqvist*, 1972], and are subject to a minimum current (Bohm) condition [*Goertz and Joyce*, 1975; *Block*, 1978]. According to this condition, for a well-defined double-layer potential drop to form, the net electron drift speed must be on the order of the electron thermal speed. The data suggest that this is the case for the event study of 9 June 1997, although it is difficult to verify since the FAST satellite does not pass through the region where the potential drop forms, but below this region. In events that have been examined during less active times (to be discussed in the next section), field-aligned currents are present, however, they are not nearly as strong as that found in the event study of the previous section. In these quite time cases the resulting field-aligned acceleration is observed to be much weaker implying that a less well-defined potential drop is formed.

[44] In the return current region, current flows in the direction opposite to that of the primary current region and thus it would be expected that a potential structure would form in the opposite sense, accelerating electrons away from the Earth [*Marklund et al.*, 1994, 1997; *Carlson et al.*, 1998b; *Ergun et al.*, 1998]. Such a structure would lead to a lack of precipitating electrons, which has been referred to as a black aurora. One-dimensional simulations of a current-

driven cold plasma with a density perturbation show that a double-layer potential structure forms which accelerates electrons and leads to electron-driven plasma instabilities [*Newman et al.*, 2001]. The simulation results are consistent with FAST electric field and particle measurements made in the midst of the return current region [*Ergun et al.*, 2001]. The accelerated electrons can excite plasma waves that could in turn then heat local ions preferably in the transverse direction, forming ion conic distributions [*Gorney et al.*, 1985]. FAST data in the return current region show accelerated electrons and ion conics that are consistent with this scenario [*Carlson et al.*, 1998b]. The net result is that along field lines in the return current at high altitudes above the auroral acceleration region, both ions and electrons would be observed streaming tailward. The physics of the acceleration for each species, however, is different. The electrons are accelerated directly by the parallel potential structure set up in the return current region and then may drive a plasma instability. The upwelling ions, on the other hand, are accelerated in a two-step process whereby first an ion conic is formed at auroral altitudes by the electron beam driven wave-particle interactions and then the mirror force by conservation of magnetic moment folds the distribution in pitch angle from transverse to parallel velocities. The upwelling electron and ion distributions observed by Polar at more equatorward latitudes in the return current region in the event study of the previous section are consistent with these types of acceleration processes (Figures 7 and 8).

[45] Although field-aligned currents are clearly a driver of field-aligned acceleration in the auroral region, there are at least two indications that they are not the only driver present in the 9 June 1997 event. The first indication from FAST (Figure 4) is the presence of an energized earthward streaming electron population at the most poleward edge of the auroral region before the satellite passes into the primary current region. Another indication is that FAST also observed earthward streaming electrons after it passed into the return current region at lower latitudes. At the same time Polar data show O^+ ion beams streaming tailward in the return current region (Figure 8). We now consider other magnetotail drivers that can account for these observations.

4.2. PSBL Beams/Quasistatic Potential Drops

[46] In the 9 June 1997 event study discussed in section 3, Polar observed high-energy earthward streaming ion beams in the PSBL that originate from the magnetotail. Such beams have been proposed as causing electrostatic shocks and parallel potential drops in the auroral zone that ultimately accelerate auroral particles [*Kan*, 1975; *Kan and Akasofu*, 1976; *Lui et al.*, 1977, 1983; *Frank et al.*, 1981; *Lyons and Evans*, 1984]. The basic mechanism involved is that the earthward streaming ion beams flowing toward the Earth represent an energy anisotropy and this anisotropy causes the plasma sheet ions and electrons to mirror at different altitudes setting up a parallel potential drop [*Alfvén and Fälthammer*, 1963; *Persson*, 1963; *Whipple*, 1977]. For the case of an ion beam streaming from the magnetotail toward the Earth, the ions mirror at an altitude lower than the electrons, setting up a potential drop oriented such that a tailward directed parallel electric field forms. This parallel electric field then accelerates electrons earthward and ions tailward. For typical PSBL ion beam energies the potential drop that results in the auroral zone can be estimated using the following formula [*Serizawa and Sato*, 1984]:

$$q\Delta\phi \approx \frac{W_{i\|}}{1 + T_i/T_e},$$

where $W_{i\|}$ represents the ion beam kinetic energy, T_i is the ion temperature, and T_e is the electron temperature. For the PSBL beams discussed in Figure 9, the ion beam kinetic energy was about 3.7 keV in one case and about 40 keV in the other case. Using an estimated ion to electron temperature ratio of $T_i/T_e \sim 7$ [e.g., *Baumjohann et al.*, 1989], the above equation gives a potential drop of $\Delta\phi \sim$ 500 V and $\Delta\phi \sim 5$ kV for the two different beam energies, respectively. Numerical simulations showed that this value can be reduced by up to 10% by wave-particle interactions [*Schriver*, 1999]. These values for the potential drop that would form in the auroral zone due the PSBL beam driver are consistent with the ~1 kV streaming energies inferred from the precipitating electrons observed by FAST and the upwelling ion beams observed by Polar.

[47] Numerical simulations have been used to examine the structure of the potential drop that forms in this situation for the case of the more energetic PSBL ion beam (40 keV). The electrostatic PIC code includes the magnetic mirror force, cold ionospheric plasma, and warm plasma that can be injected from the magnetotail plasma sheet [*Schriver*, 1999, 2003]. The simulation system is one-dimensional and aligned along the ambient magnetic field (B), which varies in strength along the simulation axis. The simulation axis is taken to be in the z direction, which is approximately equivalent to altitude and runs from $z = 0$ to $z = L$, where L is the system length. The magnetic field goes as $B \propto 1/z^3$ and the mirror force is included explicitly using $\nabla_z B$. Using a variable grid scheme with about 93,000 grids, a system length of about 20,000 km is achieved. The low-altitude end of the simulation system is set at 1000 km, and a cold ionospheric plasma is loaded in hydrostatic equilibrium. At the high-altitude end of the system (~21,000 km altitude) a population of relatively warm tenuous plasma from the magnetotail is included with an ion beam injected toward the Earth from the magnetotail. The electric field (E) is solved using Poisson's equation and is taken to be zero at the magnetospheric boundary (i.e., $E = 0$ at $z = L$). The system is kept strictly charge neutral by injecting an equal number of positive and negative charges during the simulation run. The electric potential is calculated from the electric field and is taken to be zero at the left-hand (ionospheric) boundary at $z = 0$, and is allowed to float at the right-hand boundary at $z = L$.

[48] Results are presented for a run in which the beam density relative to the background density is taken to be equal ($n_{\text{beam}} = n_{\text{background}}$). Figure 11 shows ion and electron phase space at the beginning of the simulation run on Figures 11a and 11c and at the end of the simulation run at $\omega_{pe}t = 225{,}000$ on Figures 11b and 11d. Ions are shown in Figures 11a and 11b and electrons are shown in Figures 11c and 11d. The figures show velocity (normalized to the relative species thermal speed) versus altitude in the simulation system with red representing higher-phase space density and blue lower-phase space density. In each figure the horizontal axis approximately corresponds to altitude with the Earth to the left and the magnetotail plasma sheet to

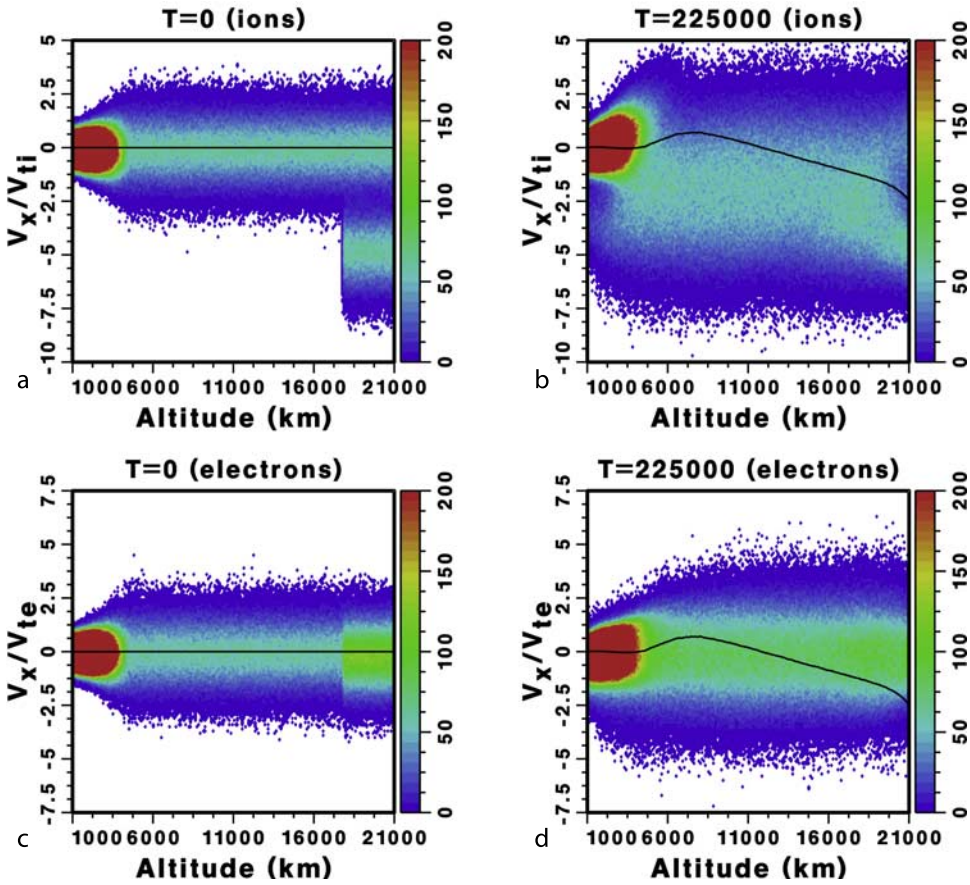

Figure 11. Ion and electron phase space snapshots at two different times are shown from an auroral particle in cell simulation in which an ion beam is injected into the system. Ions (a and b) and electrons (c and d) are shown. Velocity normalized to corresponding species thermal velocity is shown versus position along the simulation system, which is approximately along the terrestrial magnetic field. The horizontal axis has been normalized to kilometers and approximately represents altitude above the Earth. The black line across the system shows the self-consistently generated electrostatic potential in kilovolts. In each figure the Earth is to the left and the magnetotail is to the right. The initial conditions at $t = 0$ are shown in Figures 11a and 11c and the PSBL warm ion beam can be seen flowing from right to left (toward the Earth) in Figure 11a. As time proceeds in the simulation, the ion beam mirrors at a lower altitude than the PSBL electrons, leading to a quasistatic ~2.5 kV potential drop across the system above 6000 km seen in Figure 11b which shows results near the end of the run. The potential drop corresponds to a parallel electric field pointing away from the Earth over an altitude of several thousand kilometers.

the right. The black curve shows the time-averaged electric potential across the system in kilovolts. As in previous simulation runs [e.g., *Schriver*, 1999], the PSBL ions and electrons are started with the same earthward drift such that there is no net current in the plasma throughout the run. As the ions and electrons move earthward, both are decelerated by the mirror force (parallel energy converts to perpendicular energy by conservation of magnetic moment), however, on average the streaming ions can penetrate to lower altitudes than the electrons thereby setting up a potential drop of about 2.5 kV across the system above about 6000 km altitude (Figures 11b and 11d). There is a slight potential increase (~0.5 kV) that occurs below about 6000 km, which is a transient effect that moves across the system with the beam as it moves closer to the Earth. This transient effect diminishes as the beam reaches its mirror point. Previous simulations with a shorter system also produced this transient potential increase which eventually vanished [*Schriver*, 1999]. Once the main potential drop above 6000 km forms it remains relatively static over the course of the run (several seconds in real time) as long as the beam is continuously injected. If the beam driver is no longer injected into the system, the potential drop relaxes and eventually vanishes as the magnetotail ions and electrons converge to the same mirror point by the potential [*Schriver*, 1999]. The magnitude of the potential drop in the simulation is about half that estimated from the analytical formula above and is reduced by wave-particle interactions and thermal dissipation.

[49] The quasistatic potential drop that forms due to the anisotropy mirror mechanism corresponds to an electric field pointing away from the Earth, which can accelerate electrons toward the Earth and ions away from the Earth. Examples of accelerated distributions in the simulation are shown in Figure 12, with electrons at low altitude in

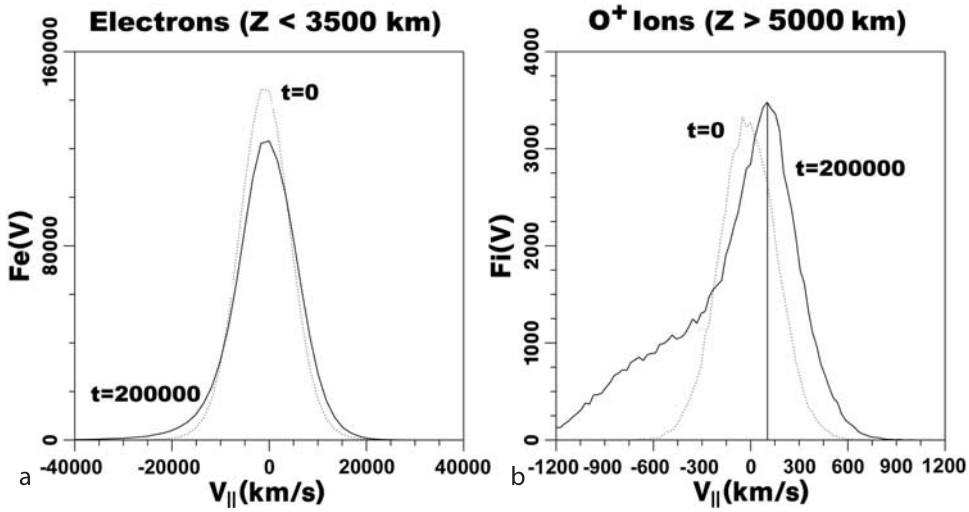

Figure 12. Electron and ion distribution functions from the simulation run shown in Figure 11 are presented. (a) The electron distribution function is shown at lower altitudes in the simulation system binned between 1000 and 3500 km. (b) The ion distribution is shown for a spatial bin between 5000 and 9000 km. In both panels the dotted line shows the initial distribution function for reference. For the low-altitude electrons (Figure 12a), a high-energy tail of particles streaming earthward (negative velocities) is created by the quasistatic parallel electric field that forms. The higher-altitude ions (Figure 12b) are accelerated away from the Earth by the quasistatic parallel electric field creating a beam-like distribution function shifted to positive (tailward directed) velocities.

Figure 12a and ionospheric ions at higher altitudes in Figure 12b. Figure 12a shows that for low-altitude electrons a high-energy tail forms on the distribution function in the earthward direction (extension in negative velocity compared to the initial distribution function). The (ionospheric) ions at higher altitudes shown in Figure 12b have also been accelerated to form a beam-like distribution compared to the initial distribution function. Wave-particle interactions have modified both distribution functions. Any beam-like features of the electron distribution have been smeared by electron plasma oscillations, while a lower-frequency ion-ion acoustic type wave has thermalized the ions somewhat giving the ion distribution a spread toward more negative parallel velocities [*Bergmann and Lotko*, 1986; *Dusenbery and Martin*, 1987]. The accelerated distributions formed in the simulation are in qualitative agreement with the precipitating electron distribution observed by FAST at lower altitudes (Figure 5) and the upgoing ion distribution observed at Polar at high altitudes (Figure 8b).

4.3. Poynting Flux/Kinetic Alfvén Waves

[50] The third magnetotail driver of auroral acceleration we consider is Poynting flux propagating toward the Earth [*Wygant et al.*, 2000; *Keiling et al.*, 2001]. This Poynting flux is in the form of Alfvén waves generated at some location down the magnetotail (at least tailward of the Polar satellite) which propagate essentially along field lines in the earthward direction. The general process is that as these magnetospheric Alfvén waves get closer to the Earth finite electron inertia effects can cause a parallel electric field component to develop that ultimately causes field-aligned electron acceleration in the auroral zone [*Hasegawa*, 1976; *Mallinckrodt and Carlson*, 1978; *Goertz and Boswell*, 1979]. Various models describing the properties of kinetic Alfvén waves have been developed for conditions found in the near-Earth auroral region [e.g., *Lysak*, 1990, 1991].

[51] Particles can be accelerated by kinetic Alfvén waves because they have a relatively low frequency ($\leq$1 Hz), and on electron timescales the parallel electric field appears to be quasistatic. Numerical models based on this premise have shown that electron acceleration can occur in the presence of kinetic Alfvén waves [*Temerin et al.*, 1986; *Kletzing*, 1994; *Thompson and Lysak*, 1996]. These models indicate that in order for these waves to induce electron acceleration their scale transverse to the geomagnetic field must be comparable to the electron skin depth. Thus the kinetic Alfvén waves have very long wavelengths (on the order of several thousand kilometers) in the field-aligned direction and relatively short wavelengths in the perpendicular direction (<10 km). For such a situation, *Temerin et al.* [1986] found that test electrons could be accelerated up to energies of several kilo electronvolts for Alfvén waves with an amplitude of about 10 mV m^{-1}. *Thompson and Lysak* [1996], also using a test particle approach, found that for an Alfvén wave with an amplitude of 0.6 mV m^{-1} (potential of 3 kV) and a static parallel potential drop of 6 kV, electrons could be accelerated to energies of several kilo electronvolts due to Landau resonance and the static potential drop.

[52] From the Polar observations the amplitude of the transverse component of the fluctuating electric field is estimated to be about 20 mV m^{-1} (see Figure 6). The parallel component would then be about 100 times less than this [*Temerin et al.*, 1986] or about 0.2 mV m^{-1}. From the Polar satellite trajectory it is estimated that the satellite moves about 500 km in the field-aligned direction. Based on these very rough estimates, the parallel potential change due to the kinetic Alfvén waves at the location of Polar would

Table 1. A List of FAST/Polar Auroral Conjunction Events[a]

	Field-Aligned Acceleration, keV			Magnetotail Driver		
Conjunction Date/Time	Electrons, keV	UFI, keV	UFE, keV	Alfvén Waves	PSBL Beam	FAC
9 June 1997/0432 UT	~1	~1	~1	X	X	X
20 July 1997/1624 UT	0.1–1		0.1–1	X		X
22 July 1997/1521 UT	0.1–1					X
24 July 1997/2040 UT	0.1–1					X
26 July 1997/1425 UT	0.1–1					X
26 July 1997/1645 UT	0.1–1					X
3 August 1997/1746 UT	~1	~0.1	~0.1	X	X	X

[a]Electron field-aligned acceleration measured by the FAST satellite is earthward directed in all cases. UFI stands for upflowing ions (away from the Earth) and UFE is for upflowing electrons, both as measured by Polar. Magnetotail drivers are observed by Polar with Alfvén waves and PSBL beams being earthward directed from the magnetotail, and FAC are field-aligned currents directed either tailward or earthward, depending on latitude.

be about 100 V. The parallel electric field component, however, probably increases closer to the Earth due to field convergence and thus a larger parallel potential drop would be present in the auroral zone below Polar. As shown by *Thompson and Lysak* [1996], if kinetic Alfvén waves are present along with a static potential drop, electrons could be accelerated to the kilo electronvolt energies observed by the FAST satellite.

[53] Most previous studies of the effects of kinetic Alfvén waves in the auroral zone have been done for electrons. How kinetic Alfvén waves might affect ions is not clear. For an electron, a wave with a frequency of 1 Hz would appear as a quasistatic wave and acceleration might occur due to the parallel electric field component. Thus for a kinetic Alfvén wave with properties that vary with altitude, coherent acceleration is possible. For the much more massive ions, however, very little acceleration is likely to occur. Unless the frequency is much lower ($\ll$1 Hz), it is difficult to see how a kinetic Alfvén wave with properties discussed above would lead to coherent ion acceleration. This is consistent with the results shown in Figure 7 whereby no upwelling ions were detected at 0423 UT to 0425 UT, which is the time corresponding to when the Alfvén wave was observed. Thus although precipitating electrons could be accelerated by kinetic Alfvén waves, tailward streaming ion beams are more likely to be caused by a parallel potential drop at lower latitudes driven either by field-aligned currents or the PSBL beams already discussed.

5. Conjunction Event Survey

[54] We now consider all of the conjunction events we have examined so far in terms of magnetotail drivers. The results are summarized in Table 1. These events include the cases in which all of the relevant particle and field data from both satellites (FAST and Polar) have been examined. The results in Table 1 are broken down by event in the first column, field-aligned acceleration in the next three columns, and the presence of the possible magnetotail drivers in the last three columns. The field-aligned acceleration columns provide the earthward electron streaming energy (at lower altitudes from FAST), upflowing ion (UFI) streaming energy (if present), and upflowing electron (UFE) streaming energy (if present), at higher altitudes from Polar. The magnetotail driver columns indicate the presence of Alfvén waves, a PSBL ion beam (earthward flow), and a field-aligned current (FAC), all as detected by Polar at high altitudes.

[55] A total of seven events have been analyzed in detail, as shown in Table 1. In all cases, the electron precipitation occurred in regions of field-aligned current (second and last columns). Two events had both upflowing ions and electrons (9 June and 3 August). The 9 June event was discussed in section 3. In both cases the electron precipitation energy was relatively high and both Alfvén wave and PSBL (ion) beam drivers were present. One case (20 July) had Alfvén waves, but no PSBL beam. Four cases had relatively weak electron precipitation and the only discernable driver was a field-aligned current. In all of the cases, FAST observed small-scale structures embedded in the larger-scale field-aligned current sheets and the field-aligned energized electrons were usually bursty, similar to the events shown in Figures 3 and 4. Also, similar to the events discussed in Figures 3 and 4, correspondence between the fine-scale current structures and the electron bursts occurred sometime, but not always.

[56] Although more events need to be examined, some general patterns appear in the results shown in Table 1 that are consistent with the physics of the auroral drivers discussed in the previous section. In the 9 June and the 3 August events, which occurred during times of enhanced magnetic activity, strong field-aligned currents, Alfvén waves, and PSBL drivers were all observed, the electron precipitation was strong (energy ~1 keV) and upwelling ions and electrons were observed. The 9 June event occurred very close to the peak of a magnetic storm (Dst = −84 nT), while the 3 August event occurred at the beginning (Dst = −40 nT) of a storm that peaked about 2–3 hours later. As already discussed, the various drivers can lead to the observed field-aligned acceleration of ions and electrons.

[57] The 20 July 1997 event occurred during moderate activity (Dst = −18), although a substorm may have been occurring at that time. Moderate amplitude Alfvén waves and weaker field-aligned currents were present and there was no PSBL beam. In this event, relatively weak electron precipitation and upwelling electrons were detected, but there was no upwelling ion beams observed. This is consistent with kinetic Alfvén waves that can accelerate electrons in the field-aligned direction, but do not accelerate ions. Since the field-aligned current was relatively weak in this case, the parallel potential drop that formed apparently was either not very strong or was not quasistatic on ion timescales. Thus somewhat weak electron precipitation and upwelling electrons could be formed in the primary and return current regions, however, no strong tailward acceleration of ions occurred.

[58] The other four events (22 July, 24 July, and two on 26 July) all occurred during quiet times with very little, if any, discernable magnetic activity. Only a very weak field-aligned current system was observed (no Alfvén waves or PSBL beams) and the resulting electron precipitation was weak. No upwelling ions or electrons were observed in these cases. Since the field-aligned current was weak,

Table 2. Summary of the Latitudinal Locations of the Different Magnetospheric Drivers and the Corresponding Field-Aligned Acceleration for the Seven Conjunction Events Examined Thus Far[a]

Latitude	Poleward Edge	Poleward	Between/ Overlapping	Equatorward
Driver	Alfvén waves	primary field-aligned current	PSBL ion beams	return field-aligned current
Field-aligned acceleration	electrons earthward	electrons earthward; ions tailward	electrons earthward; ions tailward	electrons tailward; ions tailward

[a]This table shows the results for magnetically active times. During quiet and moderately active times the PSBL ion beams were not observed. During quiet times, only the field-aligned currents were observed, the earthward electron flow was weak, and there was very little, if any, tailward plasma flow.

possibly at or below the current threshold for double-layer formation, a relatively weak potential structure was formed in the auroral zone that caused only low-energy electron precipitation and very little if any upwelling ion or electron acceleration.

6. Conclusions

[59] FAST/Polar conjunction events were used in a study to identify drivers of field-aligned auroral acceleration. The physics of the possible magnetotail drivers and auroral accelerators have been considered to help understand and interpret the satellite data. A total of seven events have been examined in detail for which FAST observed field-aligned electrons streaming earthward and Polar was in near conjunction high above the FAST satellite location. From the events examined thus far it appears that three magnetotail drivers can lead to auroral acceleration. Based on the various combinations of different types of accelerated distributions observed during different activity levels, the three driver/accelerators are listed as follows along with their characteristics.

[60] 1. Field-aligned current/quasistatic potential drop: During magnetically active times strong currents lead to strong potential drops. This results in energetic electron precipitation and upwelling ion beams in the primary current region. In the return current region a reverse potential drop accelerates electrons away from the Earth and upwelling ions are formed by the combination of wave-particle interactions and the mirror force. During moderate and quiet times a relatively weak potential drop is formed causing low-energy earthward precipitation in the primary current region and some tailward electron acceleration in the return current, but very little if any tailward ion acceleration.

[61] 2. PSBL beam/quasistatic potential drop: Present only during more active times, potential drops can be formed in the auroral region along coincident field lines where the PSBL beams are present. This potential drop can accelerate electrons earthward and ion beams tailward.

[62] 3. Poynting flux/kinetic Alfvén waves: Occurs during high and moderately active times at the highest latitude edge of the auroral zone. These waves lead to strong earthward electron acceleration and precipitation, but they do not result in tailward ion flow.

[63] The relative latitudinal location and consequences of the different drivers are summarized in Table 2, and their presence (or lack thereof) is highly dependent on magnetic activity level. Field-aligned currents were always present, however, during quiet times they become much less effective in accelerating auroral plasma. During more active times the Alfvén waves and PSBL beam were also present, and during one moderately active event only the Alfvén waves were detected (no PSBL beam). The relative latitudinal locations of the different drivers are consistent for the most part with previous observations. For example, large-amplitude Alfvén waves have been observed primarily at the poleward edge of the near-Earth plasma sheet boundary layer [*Wygant et al.*, 2000; *Keiling et al.*, 2001]. The field-aligned current structure of primary current at higher latitudes and the return current at lower latitudes is well known not only from near-Earth observations [e.g., *Iijima and Potemra*, 1976; *Carlson et al.*, 1998b], but was also observed in the PSBL at about 20 R_E down the magnetotail [*Frank et al.*, 1981]. A latitudinal dependence of the earthward streaming ion beams in the PSBL such that the highest energy beams occur at highest latitudes and beam speed decreasing with latitude has been well established [*Forbes et al.*, 1981; *Takahashi and Hones*, 1988], although the relative locations of the ion beams with respect to the field-aligned currents is unclear [*Frank et al.*, 1981]. The study here suggests that the earthward streaming ion beams of magnetotail origin overlap the primary and return current regions.

[64] Since only seven events have been examined thus far, these results must be considered as preliminary. Despite the preliminary nature of the findings thus far, however, the results follow a pattern consistent with the physics of the different magnetotail drivers. For example, when Alfvén waves were present, electrons in the auroral zone could be accelerated earthward as expected for a slowly varying (on electron timescales) parallel electric field component [*Temerin et al.*, 1986; *Kletzing*, 1994; *Thompson and Lysak*, 1996]. The formation of upwelling ions, however, requires the presence of a strong quasistatic parallel electric field, which can be supported by strong field-aligned currents or a PSBL beam. This is consistent with the general observation that ion outflow increases during magnetically active periods when the currents are strong and PSBL beams are present. During quiet times when neither the Alfvén wave driver nor the PSBL beam driver are present and the field-aligned currents are relatively weak, only low-energy electron precipitation occurs and very little, if any, ion outflow is detected.

[65] Field-aligned currents and Alfvén waves have previously been correlated observationally with field-aligned acceleration in the auroral zone and with particular electron precipitation. Ion beams of magnetotail origin as a cause of field-aligned auroral acceleration have been previously discussed theoretically, but data confirmation is lacking. This study suggests the observational possibility of ion beams as another driver of auroral acceleration. Although earthward streaming ion beams are observed at Polar in the primary current region, since both the upward directed field-aligned current and the ion beams can result in an auroral parallel potential drop that accelerates electrons earthward and ion beams tailward, it is difficult to

determine which driver is operating and accounts for the electron precipitation. On the other hand, earthward streaming ion beams are also observed by Polar in the return current region and approximately coincident with these beams are field-aligned earthward streaming electrons at FAST (see Figure 4) and tailward streaming ion beams of ionospheric origin at Polar (see Figure 8). The earthward accelerated field-aligned electrons seen by FAST in the return current region are particularly suggestive of a potential drop set up along field lines where the magnetotail ion beam driver is present since in general it is expected that electrons should be accelerated tailward by a reverse potential structure in the return current region, not earthward [e.g., *Carlson et al.*, 1998b]. Since only two such cases have been found so far in this study, however, these results are only suggestive, not definitive. Future studies will explore in more detail the spatial and temporal features of the PSBL ion beams observed at Polar as they relate to the FAST data.

[66] One of the interesting features found in the electrons observed by FAST is the bursty nature of the field-aligned acceleration (in latitude), along with small-scale structures in the current embedded in the overall large-scale field-aligned current sheets observed by both FAST and Polar. This can be seen in both Figures 3 and 4 and was found in all of the seven events discussed in Table 1. A close look at the electron peaks at 0° pitch angle (Figures 3b and 4b) and the fine-scale structures in the magnetic field (Figures 3c and 4c) show that there is correspondence some of the time, but not all of the time. It is not clear what causes the structure in electron acceleration or the magnetic field. One possibility is that density perturbations in the auroral zone (above FAST) that lead to the formation of strong potential drops in the overall field-aligned current sheet are structured and this leads to the structured electron acceleration. It is also possible that the Alfvén waves and/or PSBL ion beams are structured in latitude from their magnetospheric source region downtail. We are in the process of examining the origin of these structures by looking more closely at the satellite data and by using new large-scale auroral simulations for field-aligned currents and Alfvén waves.

[67] Although we have identified three drivers of field-aligned electron acceleration in the auroral zone, it remains to be determined how and where the magnetotail drivers originate. Field-aligned currents can form where there are flow vortices or similar types of structures [*Vasyliunas*, 1983] and are being actively examined with large-scale global magnetohydrodynamic (MHD) simulations. Both the Alfvén wave Poynting flux and the PSBL beams, since they tend to occur in the plasma sheet boundary layer during active times, indicate a possible relation to magnetic reconnection in the magnetotail. For example, a forced one-dimensional current sheet modeled using a hybrid simulation has been shown to radiate incompressible Alfvén waves [*Pritchett and Coroniti*, 1993]. Another possibility is that shear Alfvén waves are excited at the inner magnetotail boundary between cold and hot plasmas [*Lee et al.*, 2000]. The formation of the energetic earthward streaming ion beams in the PSBL has not been completely determined, with reconnection and nonadiabatic particle motion being possibilities [*Lyons and Speiser*, 1982; *Schindler and Birn*, 1987; *Ashour-Abdalla et al.*, 1991]. The appearance of the energetic PSBL beams during times of high magnetic activity might be related to a large parallel electric field that can form for highly disturbed magnetospheric conditions [*Siscoe et al.*, 2001]. It remains an unresolved problem as to how the Alfvén waves and PSBL beam drivers are reconciled with the global current system. These important issues must be considered to ultimately understand the causes of the aurora.

[68] **Acknowledgments.** The authors would like to thank E. Dors and M. El-Alaoui for useful comments and discussions related to this project. We also wish to thank C. T. Russell for the use of Polar magnetic field data, F. S. Mozer for the use of Polar electric field data, and G. Parks for the UVI data. This research was supported by NASA Guest Investigator grant NAG5-10473, NASA Geospace Sciences grant NAG5-11989, and NASA ISTP grant NAG5-11704. Computing resources were provided by the NSF National Partnership for Advanced Computing Infrastructure (NPACI).

[69] Arthur Richmond thanks David L. Newman and Michael A. Temerin for their assistance in evaluating this paper.

References

Alfvén, H., and C. G. Fälthammer, *Cosmical Electrodynamics*, Clarendon, Oxford, U. K., 1963.

Ashour-Abdalla, M., J. Berchem, J. Büchner, and L. M. Zelenyi, Large and small scale structures in the plasma sheet: A signature of chaotic motion and resonance orbits, *Geophys. Res. Lett.*, *18*, 1603, 1991.

Baumjohann, W., G. Paschmann, and C. A. Cattell, Average plasma properties in the central plasma sheet, *J. Geophys. Res.*, *94*, 6597, 1989.

Bergmann, R., and W. Lotko, Transition to unstable ion flow in parallel electric fields, *J. Geophys. Res.*, *91*, 7033, 1986.

Blake, J. B., et al., CEPPAD (Comprehensive Energetic Particle and Pitch Angle Distribution) on Polar, *Space Sci. Rev.*, *71*, 563, 1995.

Block, L. P., Potential double layers in the ionosphere, *Cosmic Electrodyn.*, *3*, 349, 1972.

Block, L. P., A double layer review, *Astrophys. Space Sci.*, *55*, 59, 1978.

Carlqvist, P., On the formation of double layers in plasmas, *Cosmic Electrodyn.*, *3*, 377, 1972.

Carlson, C. W., R. F. Pfaff, and J. G. Watzin, The Fast Auroral Snapshot (FAST) mission, *Geophys. Res. Lett.*, *25*, 2013, 1998a.

Carlson, C. W., et al., FAST observations in the downward current region: Energetic upgoing electron beams, parallel potential drops, and ion heating, *Geophys. Res. Lett.*, *25*, 2017, 1998b.

Chiu, Y. T., and J. M. Cornwall, Electrostatic model of a quiet auroral arc, *J. Geophys. Res.*, *85*, 543, 1980.

Chiu, Y. T., J. M. Cornwall, and M. Schulz, Effects of auroral-particle anisotropies and mirror forces on high-latitude electric fields, in *Physics of Auroral Arc Formation*, *Geophys. Monogr. Ser.*, vol. 25, edited by S.-I. Akasofu and J. R. Kan, 234 pp., AGU, Washington, D. C., 1981.

Christensen, A. B., L. R. Lyons, J. H. Hecht, G. G. Sivjee, R. R. Meier, and D. G. Strickland, Magnetic field-aligned electric field acceleration and characteristics of the optical aurora, *J. Geophys. Res.*, *92*, 6163, 1987.

DeCoster, R. J., and L. A. Frank, Observations pertaining to the dynamics of the plasma sheet, *J. Geophys. Res.*, *84*, 5099, 1979.

Dusenbery, P. B., and R. F. Martin Jr., Generation of broadband turbulence by accelerated auroral ions: 1, Parallel propagation, *J. Geophys. Res.*, *92*, 3261, 1987.

Eastman, T. E., L. A. Frank, W. K. Peterson, and W. Lennartsson, The plasma sheet boundary layer, *J. Geophys. Res.*, *89*, 1553, 1984.

Elphic, R. C., et al., The auroral current circuit and field-aligned currents observed by FAST, *Geophys. Res. Lett.*, *25*, 2033, 1998.

Ergun, R. E., et al., FAST satellite observations of electric field structures in the auroral zone, *Geophys. Res. Lett.*, *25*, 2025, 1998.

Ergun, R. E., C. W. Carlson, J. P. McFadden, and F. S. Mozer, Parallel electric fields in discrete arcs, *Eos Trans. AGU*, *81*, Fall Meet. Suppl., F1026, 2000.

Ergun, R. E., L. Andersson, Y. Su, C. W. Carlson, J. P. McFadden, F. S. Mozer, D. L. Newman, M. V. Goldman, and R. J. Strangeway, Direct observation of parallel electric fields of the aurora, *Eos Trans. AGU*, *82*, Fall Meet Suppl., F1064, 2001.

Evans, D. S., Precipitating electron fluxes formed by a magnetic field aligned potential difference, *J. Geophys. Res.*, *79*, 2853, 1974.

Forbes, T. G., E. W. Hones Jr., S. J. Bame, J. R. Asbridge, G. Paschmann, N. Sckopke, and C. T. Russell, Evidence for the tailward retreat of a magnetic neutral line in the magnetotail during substorm recovery, *Geophys. Res. Lett.*, *8*, 261, 1981.

Frank, L. A., Plasmas in the Earth's magnetotail, *Space Sci. Rev.*, *42*, 211, 1985.
Frank, L. A., and K. L. Ackerson, Observations of charged particle precipitation into the auroral zone, *J. Geophys. Res.*, *76*, 3612, 1971.
Frank, L. A., K. L. Ackerson, and R. P. Lepping, On hot tenuous plasmas, fireballs, and boundary layers in the Earth's magnetotail, *J. Geophys. Res.*, *81*, 5859, 1976.
Frank, L. A., R. L. McPherron, R. J. DeCoster, B. G. Burek, K. L. Ackerson, and C. T. Russell, Field aligned currents in the Earth's magnetotail, *J. Geophys. Res.*, *86*, 687, 1981.
Ghielmetti, A. G., R. G. Johnson, R. D. Sharp, and E. G. Shelley, The latitudinal, diurnal, and altitudinal distributions of upward flowing energetic ions of ionospheric origin, *Geophys. Res. Lett.*, *5*, 59, 1978.
Goertz, C. K., and R. W. Boswell, Magnetosphere-ionosphere coupling, *J. Geophys. Res.*, *84*, 7239, 1979.
Goertz, C. K., and G. Joyce, Numerical simulation of the plasma double layer, *Astrophys. Space Sci.*, *32*, 165, 1975.
Gorney, D. J., J. A. Clarke, D. Croley, J. Fennel, J. Luhmann, and P. Mizera, The distribution of ion beams and conics below 8000 km, *J. Geophys. Res.*, *86*, 83, 1981.
Gorney, D. J., Y. T. Chiu, and D. R. Croley Jr., Trapping of ion conics by downward parallel electric fields, *J. Geophys. Res.*, *90*, 4205, 1985.
Haerendel, G., Field-aligned currents in the Earth's magnetosphere, in *Physics of Magnetic Flux Ropes*, *Geophys. Monogr. Ser.*, vol. 58, edited by C. T. Russell, E. R. Priest, and L. C. Lee, 539 pp., AGU, Washington, D. C., 1990.
Harvey, P., et al., The electric field instrument on the Polar satellite, *Space Sci. Rev.*, *71*, 583, 1995.
Hasegawa, A., Particle acceleration by MHD surface wave and formation of aurora, *J. Geophys. Res.*, *81*, 5083, 1976.
Hoffman, R. A., and D. S. Evans, Field-aligned electron bursts at high latitude observed by Ogo 4, *J. Geophys. Res.*, *73*, 6201, 1968.
Hones, E. W., Jr., J. R. Asbridge, S. J. Bame, M. D. Montgomery, S. Singer, and S.-I. Akasofu, Measurements of magnetotail plasma flow make with Vela 4B, *J. Geophys. Res.*, *77*, 5503, 1972.
Hultqvist, B., H. Borg, W. Reidler, and P. Chistopherson, Observations of a magnetic field-aligned anisotropy for 1 and 6 keV positive ions in the upper ionosphere, *Planet. Space Sci.*, *19*, 279, 1971.
Iijima, T., and T. A. Potemra, The amplitude distribution of field-aligned currents at northern high latitudes observed by TRIAD, *J. Geophys. Res.*, *81*, 2165, 1976.
Kan, J. R., Energization of auroral electrons by electrostatic shock waves, *J. Geophys. Res.*, *80*, 2089, 1975.
Kan, J. R., and S.-I. Akasofu, Energy source and mechanisms for accelerating the electrons and driving the field-aligned currents of the discrete auroral arc, *J. Geophys. Res.*, *81*, 5123, 1976.
Keiling, A., J. R. Wygant, C. Cattell, M. Johnson, M. Temerin, F. S. Mozer, C. A. Kletzing, J. Scudder, and C. T. Russell, Properties of large electric fields in the plasma sheet at 4–7 RE measured with Polar, *J. Geophys. Res.*, *106*, 5779, 2001.
Kennel, C. F., Consequences of a magnetospheric plasma, *Rev. Geophys.*, *7*, 379, 1969.
Kennel, C., and H. Petschek, Limit on stable trapped particle fluxes, *J. Geophys. Res.*, *71*, 1, 1966.
Kletzing, C. A., Electron acceleration by kinetic Alfvén waves, *J. Geophys. Res.*, *99*, 11,095, 1994.
Kletzing, C. A., and J. D. Scudder, Auroral-plasma sheet electron anisotropy, *Geophys. Res. Lett.*, *26*, 971, 1999.
Knight, S., Parallel electric fields, *Planet. Space Sci.*, *21*, 741, 1973.
Lee, D. H., R. L. Lysak, and Y. Song, Generation of field-aligned currents in the near-Earth magnetotail, *Eos Trans. AGU*, *81*, Fall Meet. Suppl., F1051, 2000.
Lemaire, J., and M. Scherer, Ionosphere-plasmasheet field-aligned currents and parallel electric fields, *Planet. Space Sci.*, *22*, 1485, 1974.
Lui, A. T. Y., E. W. Hones Jr., F. Yasuhara, S.-I. Akasofu, and S. J. Bame, Magnetotail plasma flow during plasma sheet expansions: Vela 5 and 6 and IMP 6 observations, *J. Geophys. Res.*, *82*, 1235, 1977.
Lui, A. T. Y., T. E. Eastman, D. J. Williams, and L. A. Frank, Observation of ion streaming during substorms, *J. Geophys. Res.*, *88*, 8853, 1983.
Lyons, L. R., and D. S. Evans, An association between discrete auroral and energetic particle boundaries, *J. Geophys. Res.*, *89*, 2395, 1984.
Lyons, L. R., and T. W. Speiser, Evidence for current sheet acceleration in the geomagnetic tail, *J. Geophys. Res.*, *87*, 2276, 1982.
Lyons, L. R., T. Nagai, G. T. Blanchard, J. C. Samson, T. Yamamoto, T. Mukai, A. Nishida, and S. Kokubun, Association between Geotail plasma flows and auroral poleward boundary, *J. Geophys. Res.*, *104*, 4485, 1999.
Lysak, R. L., Auroral electrodynamics with current and voltage generators, *J. Geophys. Res.*, *90*, 4178, 1985.
Lysak, R. L., Electrodynamic coupling of the magnetosphere and ionosphere, *Space Sci. Rev.*, *52*, 33, 1990.
Lysak, R. L., Feedback instability of the ionospheric resonant cavity, *J. Geophys. Res.*, *96*, 1553, 1991.
Lysak, R. L., The relationship between electrostatic shocks and kinetic Alfvén waves, *Geophys. Res. Lett.*, *25*, 2089, 1998.
Mallinckrodt, A. J., and C. W. Carlson, Relations between transverse electric fields and field-aligned currents, *J. Geophys. Res.*, *83*, 1426, 1978.
Marklund, G., L. Blomberg, C. G. Fälthammer, and P.-A. Lindqvist, On intense diverging electric fields associated with black aurora, *Geophys. Res. Lett.*, *21*, 1859, 1994.
Marklund, G., T. Karlsson, and J. Clemmons, On low-altitude particle acceleration and intense electric fields and their relationship to black aurora, *J. Geophys.*, 102, 1997.
McIlwain, C. E., Direct measurements of particles producing visible auroras, *J. Geophys. Res.*, *65*, 73, 1960.
Möbius, E., F. M. Ipavich, M. Scholer, G. Gloeckler, D. Hovestadt, and B. Klecker, Observation of nonthermal ion layer at the plasma sheet boundary during substorm recovery, *J. Geophys. Res.*, *85*, 5143, 1980.
Mozer, F. S., C. Carlson, M. Hudson, R. Torbert, B. Parady, J. Yatteau, and M. Kelley, Observations of paired electrostatic shocks in the polar magnetosphere, *Phys. Rev. Lett.*, *38*, 292, 1977.
Newman, D. L., M. V. Goldman, R. E. Ergun, and A. Mangeney, Formation of double layers and electron holes in a current-driven space plasma, *Phys. Rev. Lett.*, *87*, 2555001-1, 2001.
Persson, H., Electric field along a magnetic line of force in a low density plasma, *Phys. Fluids*, *6*, 1756, 1963.
Pritchett, P. L., and F. V. Coroniti, A radiating one dimensional current sheet configuration, *J. Geophys. Res.*, *98*, 15,355, 1993.
Rees, M. H., and D. Luckey, Auroral electron energy derived from ratio of spectroscopic emissions, 1, Model computations, *J. Geophys. Res.*, *79*, 5181, 1974.
Reiff, P. H., H. L. Collin, E. G. Shelley, J. L. Burch, and J. D. Winningham, Heating of upflowing ionospheric ions on auroral field lines, in *Ion Acceleration in the Magnetosphere and Ionosphere*, *Geophys. Monogr. Ser.*, vol. 38, edited by T. Chang, pp. 83, AGU, Washington, D. C., 1986.
Reiff, P. H., H. L. Collin, J. D. Craven, J. L. Burch, J. D. Winningham, E. G. Shelley, L. A. Frank, and M. A. Friedman, Determination of auroral electrostatic potentials using high and low altitude particle distributions, *J. Geophys. Res.*, *93*, 7441, 1988.
Russell, C., R. C. Snare, J. D. Means, D. Pierce, D. Dearborn, M. Larson, G. Barr, and G. Le, The GGS/Polar magnetic fields investigation, *Space Sci. Rev.*, *71*, 563, 1995.
Schindler, K., and J. Birn, On the generation of field-aligned plasma flow at the boundary of the plasma sheet, *J. Geophys. Res.*, *92*, 95, 1987.
Schriver, D., Particle simulation of the auroral zone showing parallel electric fields, waves and plasma acceleration, *J. Geophys. Res.*, *104*, 14,655, 1999.
Schriver, D., Simulating an inhomogeneous plasma system: Variable grids and boundary conditions, in *Space Plasma Simulation, Lecture Notes in Physics*, vol. 615, edited by J. Büchner, C. T. Dum, and M. Scholer, Springer-Verlag, New York, 2003.
Schriver, D., M. Ashour-Abdalla, R. Treumann, M. Nakamura, and L. M. Kistler, The lobe to plasma sheet boundary layer transition: Theory and observations, *Geophys. Res. Lett.*, *17*, 2027, 1990.
Scudder, J. D., et al., Hydra—A 3-dimensional electron and ion hot plasma instrument for the Polar spacecraft of the GGS mission, *Space Sci. Rev.*, *71*, 459, 1995.
Serizawa, Y., and T. Sato, Generation of large scale potential difference by currentless plasma jets along the mirror field, *Geophys. Res. Lett.*, *11*, 595, 1984.
Sharp, R. D., R. G. Johnson, and E. G. Shelley, Observation of an ionospheric acceleration mechanism producing energetic (keV) ions primarily normal to the geomagnetic field direction, *J. Geophys. Res.*, *82*, 3324, 1977.
Shelley, E. G., R. D. Sharp, and R. G. Johnson, Satellite observations of an ionospheric acceleration mechanism, *Geophys. Res. Lett.*, *3*, 654, 1976.
Siscoe, G. L., G. M. Erickson, B. U. O. Sonnerup, N. C. Maynard, K. D. Siebert, D. R. Weimer, and W. W. White, Global role of $E_{||}$ in magnetopause reconnection: An explicit demonstration, *J. Geophys. Res.*, *106*, 13,015, 2001.
Stenbaek-Nielsen, H. C., T. J. Hallinan, D. L. Osborne, J. Kimball, C. Chaston, J. McFadden, G. Delory, M. Temerin, and C. W. Carlson, Aircraft observations conjugate to FAST: Auroral arc thicknesses, *Geophys. Res. Lett.*, *25*, 2033, 1998.
Swift, D. W., On the formation of auroral arcs and acceleration of auroral electrons, *J. Geophys. Res.*, *80*, 2096, 1975.
Takahashi, K., and E. W. Hones Jr., ISEE 1 and 2 observations of ion distributions at the plasma sheet-tail lobe boundary, *J. Geophys. Res.*, *93*, 8558, 1988.

Temerin, M. A., J. McFadden, M. Boehm, C. W. Carlson, and W. Lotko, Production of flickering aurora and field-aligned electron flux by electromagnetic ion cyclotron waves, *J. Geophys. Res.*, *91*, 5769, 1986.

Thompson, B. J., and R. L. Lysak, Electron acceleration by inertial Alfvén waves, *J. Geophys. Res.*, *101*, 5359, 1996.

Torr, M. R., et al., A far ultraviolet imager for the international solar-terrestrial physics mission, *Space Sci. Rev.*, *71*, 329, 1995.

Tsyganenko, N. A., A magnetospheric magnetic field model with a warped tail current sheet, *Planet. Space Sci.*, *37*, 5, 1989.

Tsyganenko, N. A., and D. P. Stern, Modeling the global magnetic field of the large-scale Birkeland current systems, *J. Geophys. Res.*, *101*, 27,187, 1996.

Vasyliunas, V. M., Fundamentals of current description, in *Magnetospheric Currents*, *Geophys. Monogr. Ser.*, vol. 28, edited by T. A. Potemra, 63 pp., AGU, Washington, D. C., 1983.

Whipple, E. C., The signature of parallel electric fields in a collisionless plasma, *J. Geophys. Res.*, *82*, 1525, 1977.

Wygant, J. R., et al., Polar spacecraft based comparisons of intense electric fields and Poynting flux near and within the plasma sheet-tail lobe boundary to UVI images: An energy source for the auroral, *J. Geophys. Res.*, *106*, 18,675, 2000.

M. Ashour-Abdalla, R. L. Richard, D. Schriver, and R. J. Strangeway, Institute of Geophysics and Planetary Physics, University of California at Los Angeles, 3845 Slichter Hall, 405 Hilgard Avenue, Los Angeles, CA 90095-1567, USA. (mabdalla@igpp.ucla.edu; rrichard@igpp.ucla.edu; dave@igpp.ucla.edu; strange@igpp.ucla.edu)

Y. Dotan, Aerospace Corporation, 2350 East El Segundo Boulevard, Los Angeles, CA 90009, USA. (yaniv.dotan@earo.org)

C. Klezting, Department of Physics and Astronomy, University of Iowa, Iowa City, IA 52242, USA. (cak@delta.physics.uiowa.edu)

J. Wygant, School of Physics and Astronomy, University of Minnesota, Minneapolis, MN 55455, USA. (wygant@belka.space.umn.edu)